



UPPSALA
UNIVERSITET

UPTEC W 24043

Examensarbete 30 hp

Augusti 2024

Projected changes in sea-effect snowfall over the Swedish Baltic Sea region

Results from a high-resolution regional climate model

Siri Westerblom



UPPSALA
UNIVERSITET

Projected changes in sea-effect snowfall over the Swedish Baltic Sea region – Results from a high-resolution regional climate model

Siri Westerblom

Abstract

Extreme weather can cause large disruptions to both natural and human systems and the recurrence and intensity of such events can be affected by climate change. One phenomenon that can lead to hazardous snowstorms over coastal regions is sea-effect snowfall, which can arise during the winter over large, ice-free bodies of water. A warmer climate may lead to shorter winters and fewer days of snowfall but also less sea ice and higher precipitation rates, which can impact this phenomenon. The aim of this thesis was to investigate changes in occurrence and intensity of sea-effect snowfall over the Swedish Baltic Sea region in a future warmer climate and to study the impact of using a high resolution, convection-permitting climate model in this area.

This was done by analyzing simulations from the HARMONIE-Climate (HCLIM) regional climate model system with boundary data from reanalysis and four CMIP6 global climate models. Future climate was simulated for mid and end of the 21st century using the SSP370 emission scenario. Horizontal grid resolutions of 3 km and 12 km were compared. Results indicate that the number of sea-effect snowfall events will decrease in a future warmer climate, especially in the southern parts of the Baltic Sea. The total precipitation rates during these events will likely increase. The snowfall rates will decrease over water but the effect over the coastal regions remains unclear, though some signs of increasing intensity of events in the north exist. In relation to the course model resolution the high-resolution model identified more days with sea-effect snowfall, was associated with, on average, lower precipitation rates but higher extreme and short-term intensities. Compared to available observations and reanalysis both model resolutions showed similar performance in the simulation of precipitation for selected snowband days.

Keywords: Lake-effect snowfall, sea-effect snowfall, convective snowbands, climate change, regional climate model, HCLIM, Baltic Sea

Teknisk-naturvetenskapliga fakulteten

Uppsala universitet, Utgivningsort Uppsala

Handledare: Petter Lind Ämnesgranskare: Gabriele Messori

Examinator: Johan Arnqvist



Referat

Extremväder kan orsaka stora störningar i både naturliga och mänskliga system, förekomster och intensitet av sådana händelser kan komma att påverkas av klimatförändringar. Ett fenomen som kan leda till kraftiga snöstormar över kustområden är snökanoner, dessa kan bildas under vinterhalvåret över stora isfria vattenmassor. Ett varmare klimat kan leda till kortare vintrar och färre dagar med snöfall men även mindre havsis och högre nederbördsintensiteter vilket kan påverka detta fenomen. Syftet med detta examensarbete var att undersöka förändringar i förekomst och intensitet av snökanoner över den svenska Östersjöregionen i ett framtida varmare klimat. Men också för att studera effekten av att använda en högupplöst regional klimatmodell inom detta område.

Detta undersöktes med hjälp av HARMONIE-Climate (HCLIM) regionala modellsystem driven med randvillkor från återanalys och fyra globala klimatmodeller. Framtida klimat simulerades för mitten och slutet av 2000-talet för utsläppsscenario SSP370. Horisontella modellupplösningar på 3 km och 12 km jämfördes. Resultaten visar att antalet snökanoner troligt kommer att minska i ett framtida varmare klimat, särskilt i de södra delarna av Östersjön. Den totala nederbörden under dessa händelser kommer sannolikt att öka. Snöfraktionen och snöfallsmängder kommer att minska över vatten, men effekten över kustområdena är fortfarande tvetydig, dock tyder vissa tecken på ökade intensiteter över land i norr. Högre modellupplösning ledde till fler identifierade fall av snökanoner, generellt lägre ackumulerade nederbörds mängder men högre extrema och kortsiktiga nederbördsintensiteter. Vid jämförelse med tillgängliga observationer och återanalys uppvisar båda modellupplösningarna liknande prestanda vid simulering av nederbörd för utvalda snökanonsdagar.

Nyckelord: Snökanoner, sjösnö, klimatförändring, regional klimatmodell, HCLIM, Östersjön

Teknisk-naturvetenskapliga fakulteten

Uppsala universitet, Utgivningsort Uppsala

Handledare: Petter Lind Ämnesgranskare: Gabriele Messori

Examinator: Johan Arnqvist

Förord

Med detta examensarbete avslutar jag mina studier på civilingenjörsprogrammet i miljö- och vattenteknik på Uppsala universitet och Sveriges lantbruksuniversitet. Min handledare var Petter Lind, klimatforskare på Rossby center, SMHI. Min ämnesgranskare var Gabriele Messori, professor vid institutionen för geovetenskaper, luft-, vatten och landskapslära; meteorologi, Uppsala universitet.

Jag vill rikta ett stort tack till dig Petter för all hjälp i det dagliga arbetet, bra bollplank och skrattattacker under tidens gång. Tack också till Erik Kjellström och Helena Martins som tog emot mig och fick mig att vilja göra just detta examensarbete. Tack till resten av det härliga gänget på Rossby, det har varit trevligt att få sitta på ert kontor och bli inkluderad i gänget. Tack även till dig Gabriele för stöd och bra feedback. Tack till min sambo, Axel ditt tålamod är enormt. Till sist vill jag även tacka alla vänner och kursare som förgyllt min studietid här i Uppsala.

Populärvetenskaplig Sammanfattning

Väder och olika meteorologiska fenomen påverkar vardagen i både naturliga och mänskliga system. Vissa typer av händelser som kallas för extremväder kan leda till mer allvarliga effekter på skog, bebyggelse, infrastruktur och så vidare. Ett sådant fenomen kallas för snökanoner och är huvudfokuset för denna rapport.

Snökanoner är långa men smala band av moln som kan leda till kraftiga snöstormar på lokala platser. De kan uppstå under vinterhalvåret när väldigt kalla luftmassor färdas över en stor, relativt varm och isfri vattenmassa som exempelvis Väneren och Vättern eller Östersjön. När detta sker så blir det en väldigt skarp temperaturgradient mellan vattenytan och den ovanliggande luften. Detta sätter igång flöden av fukt och värme från vattnet till luften. Luften närmast vattenytan är nu varmare än luften ovan och börjar därför stiga eftersom varm luft har större flytkraft än kall luft. Vi får alltså en värmetransport i vertikal led som kallas konvektion. När denna varma och fuktiga luft stiger så kyls den succesivt av med höjden och tillslut börjar vattenångan att kondensera, det bildas moln. Om det samtidigt är relativt höga vindhastigheter och liten förändring av vindriktningen med höjden så kan detta organiseras i långsmala band av intensiv konvektion som färdas och sträcker ut sig över vattenytan. När snökanonerna sedan når kusten och den kalla marken så avtar värmeflödet underifrån och vi får en relativt abrupt nedbrytning av strukturen. Därför når snöfallet sällan långt inland. Ett extremfall av snökanoner som skett i Sverige träffade kusten vid Gävle under vintern 1998. Under endast fyra dagar steg snödjupet från 1 till 131 cm vilket stängde ner hela staden och ledde till att militär undsättning behövde kallas in.

Med allt snabbare klimatförändringar som observeras ökar behovet av att undersöka hur detta kan påverka väder och olika fenomen i framtiden. Det är ett viktigt första steg för att kunna anpassa våra samhällen och minska konsekvenserna. Dessa klimatförändringar kan studeras med hjälp av klimatmodeller där man delar in hela jorden i ett rutnät och sen simulerar vädret numeriskt för långa tidsperioder i varje ruta. Det finns globala modeller som simulerar hela jordklotet och regionala modeller som har högre upplösning (flera och mindre rutor på samma area jämfört med den globala) och högre detaljeringsgrad. Detta kräver mer datorkapacitet och minne och de kan därför bara kan simuleras över en begränsad yta, exempelvis Europa. Den regionala modellen kräver då indata från den globala modellen på kanterna av den begränsade ytan. På så sätt ger den regionala modellen en inzoomad version av den globala simuleringen vilket brukar kallas för nedskalning. Modellerna kan simulera vårt nutida klimat och framtida klimat med olika grad av uppvärmning, växthusgashalter och mänsklig påverkan på systemen, även kallat för utsläppsscenarier.

I Östersjöområdet spås i framtiden klimatet att bli varmare, speciellt under vinterperioderna och i de norra delarna, och även leda till ökade nederbördsintensiteter. Detta skulle kunna begränsa uppkomsten av snökanoner i framtiden då varmare temperaturer leder till färre dagar med snöfall. Men det skulle även kunna gynna snökanoner då varmare temperaturer leder till mindre is på vattnet vilket möjliggör dess uppkomst. Med större nederbörds mängder generellt är det även möjligt att framtida snökanoner kommer med mer extrema snöfall. Syftet med denna rapport var att undersöka förändringar av förekomst och intensitet av snökanoner i den svenska Östersjöregionen i ett framtida varmare klimat. Men också att utvärdera vilken påverkan på resultatet som klimatmodellens upplösning har. Kan en mer högupplöst modell som har en mer fullständig beskrivning av konvektion förbättra simuleringen av detta lokala fenomen?

För att studera det här har en regional klimatmodell som heter HCLIM använts med två olika upplösningar, rutnät på 3 x 3 km och 12 x 12 km. Historiskt klimat och ett framtida varmare klimat med ett utsläppsscenario som kallas SSP370 har simulerats.

Resultatet av studien visar att antalet snökanoner i Östersjöregionen högst troligt kommer att minska i framtiden längs hela den svenska östkusten. Detta på grund av färre dagar med tillräckligt kalla temperaturer för snöfall. Den totala nederbörden för framtida snökanoner prognostiseras att öka i medeltal. Snömängderna kommer minska över hav men ökar potentiellt över land, framförallt i norr. När man jämför resultat av de olika modellupplösningarna simulerar den högupplösta modellen fler fall av snökanoner. Den resulterade även i högre extremvärden och kraftigare kortvariga intensiteter av nederbörd, vilket ofta kännetecknar konvektiv nederbörd så som snökanoner. Vid jämförelser av tillgängliga referensdata för nederbörd uppvisar båda modeller liknande prestanda.

List of abbreviations

ABL	Atmospheric Boundary Layer
ALADIN	Aire Limitée Adaptation dynamique Développement InterNational
AROME	Applications of Research to Operations at MEscale
CMIP	Coupled Model Intercomparison Project
ECMWF	European Centre for Medium-Range Weather Forecasts
ERA-Interim	ERA-Interim
GCM	Global Climate Model
GridClim	SMHI Gridded Climatology
HARMONIE	The HIRLAM–ALADIN Regional Mesoscale Operational NWP in Europe
HCLIM	HARMONIE Climate (regional model system)
HCLIM3	HCLIM-AROME, with 3 x 3 km horizontal resolution
HCLIM12	HCLIM-ALADIN, with 12 x 12 km horizontal resolution
HCLIM12-ENS	Signifying the ensemble results of all GCMs downscaled by HCLIM12
HIRLAM	The High Resolution Limited Area Model
NGCD	Nordic Gridded Climate Dataset
NWP	Numerical Weather Prediction
RCM	Regional Climate Model
SSP	Shared Socioeconomic Pathways
SST	Sea Surface Temperature
SST-T850	Temperature difference between the sea surface temperature and air temperature at the 850 hPa level, often referred to as the temperature gradient

Contents

1	Introduction	1
1.1	Aim	1
2	Background	2
2.1	Convective snowbands	2
2.1.1	Formation of snowbands	2
2.1.2	Recent studies	4
2.2	Numerical weather and climate models	5
3	Data and method	6
3.1	Model description and data	6
3.2	Validation data	8
3.3	Methodology	8
3.3.1	Detection of snowband days	8
3.3.2	Analysis	9
4	Results	12
4.1	Present-day climate	12
4.1.1	Impact of model resolution	16
4.2	Future projections	20
5	Discussion	25
5.1	Present-day climate	25
5.2	Impact of model resolution	26
5.3	Future projections	27
6	Conclusion	29
7	References	30
	Appendices	32
A	Frequency of events	32
B	Ensemble results disregarding HCLIM12-MIROC6	33
C	Precipitation	35
D	Meteorological Parameters	39

1 Introduction

Weather and various meteorological phenomena affect natural and human systems on a daily basis. Certain types of events can have bigger impact than others and one of those is the main focus of this thesis. Sea- or lake-effect snowfall, also called convective snowbands, are convective clouds organized into long but narrow bands which under specific conditions cause heavy snowfall both over sea and coastal regions such as the Swedish east coast (SMHI 2023b). These bands form over open water during the cold season and sometimes lead to hazardous conditions such as the case of Gävle, Sweden, in December 1998. During this event the snow depth increased by 130 cm in less than four days causing huge disruptions in the traffic, shut down of schools and railway system, power outages etc. In the end these high-impact events can amount to large societal costs and the bill for direct effects of the Gävle case was reported by the municipality in spring of 1999 as 48.2 million SEK (Hedman 1999).

The ongoing rapid and widespread observed climate change raises the question of how weather and phenomena like this might shift in the future. Making use of climate model simulations of future scenarios to investigate potential changes in occurrence and intensity of such events is a necessary step to facilitate adaptation of society and mitigate consequences. The extent and magnitude of climate change will depend on policy implementations and their effect on greenhouse gas emissions, land use, etc. However, all of the latest generation of emission scenarios for the future show a warming towards mid and end of 21st century compared to 1850-1900 (IPCC 2023). The increase in global mean temperature will further affect other aspects of the weather and the climate system. For example, the occurrence of extreme weather will likely increase and the global water cycle intensify in relation to the warming (IPCC 2023). Using regional climate models (RCMs) the current projections for the Baltic Sea area indicate warmer temperatures, particularly during the winter season and in northern regions, as well as increasing precipitation amounts (Christensen & Kjellström 2018). This in turn leading to higher sea surface temperatures (SST) and less sea ice which opens up the possibility for more frequent and intense convective snowfall events in the future. At the same time, increasing temperatures will lead to a shorter winter season and less snow on the whole, which may be a limiting factor.

1.1 Aim

The aim of this project was to outline how convective snowbands have varied in the last decades and how they may change in future scenarios. This was done using the HCLIM regional climate model framework with both 12 km and 3 km horizontal grid resolutions to evaluate the potential benefits of a high-resolution, convection-permitting model in this study area. The following questions of interest were the focus of this thesis:

How will convective snowband events over the Swedish Baltic Sea region change in a future, warmer climate regarding both frequency and intensity?

How does a convection-permitting regional climate model impact the results and simulations of convective snowbands?

2 Background

2.1 Convective snowbands

Convective snowbands or sea-effect snowfall is a mesoscale (horizontal scale of a couple to several hundred kilometers) precipitation event which can occur during the cold season, mainly in the middle and high latitudes. This phenomena can be seen on radar or satellite images as long, narrow, singular or multiple bands of clouds aligned with the direction of the wind, typically staying within the first 2 km of the atmosphere (Fujisaki-Manome et al. 2022), see example in Figure 1 . Depending on the meteorological conditions snowbands of different type and intensity can form. From shorter-duration events with loosely organized bands and light snow showers to more stationary, highly organised cloud structures possibly leading to intense snow storms lasting several days (Niziol 1987). Due to the slim nature of the bands, usually not wider than 5 km, the impact areas are generally quite small and leading to very local snowfall. They appear in different places where the right conditions can occur and have for example been extensively studied at the Great lakes in North America (e.g. Holroyd 1971; Niziol 1987, Sea of Japan (e.g Steenburgh & Nakai 2020) and the Baltics (e.g. Andersson & Nilsson 1990; Olsson et al. 2020).

In instances where convective snowbands become intense and/or stationary, they can lead to large accumulations of snow, affecting various parts of our societies. Due to e.g. snowdrifts, fallen trees or slippery conditions impacts can be seen on all types of transportation. Leading to decreased accessibility, causing problems to vital societal functions and increased risks for accidents (MSB 2022). Large amounts of snow can also cause damages to power lines and result in power outages. The snow load, meaning the force exerted by the accumulated snow on a surface, can in these cases become substantial and cause roofs to collapse. These effects needs to be taken into account when designing cities to ensure infrastructure for snow removal and when setting regulations for load-bearing constructions (MSB 2022).

2.1.1 Formation of snowbands

Convective snowbands usually form when a cold air mass cross over a warmer, ice free sea. The large temperature difference between the water surface and overlying air lead to unstable conditions and trigger heat and moisture fluxes from the water to the air and convective cells are formed (Andersson & Nilsson 1990). Holroyd (1971) found empirically that for convective snowbands to occur the temperature difference between the water surface and the air at 850 hPa need to be greater than 13 °C. This corresponds approximately to the dry adiabatic lapse rate, $\Gamma_d = -9.8 K/km$, which is the temperature change with altitude in a dry air parcel if no heat is exchanged with the surrounding air. A larger temperature decrease with height would then indicate absolute unstable conditions which promote vertical movements. The rising air then cools gradually with height, eventually reaching the lifted condensation level where the temperature of the air parcel has dropped to the dew point temperature, becomes saturated and clouds start to form (Stull 2017). When the air moves in over land or ice the heat and moisture fluxes weaken significantly from the surface, which results in convective bands breaking down swiftly after reaching the coast. Precipitation maxima is often seen over the sea close to the coastline (Andersson & Nilsson 1990).

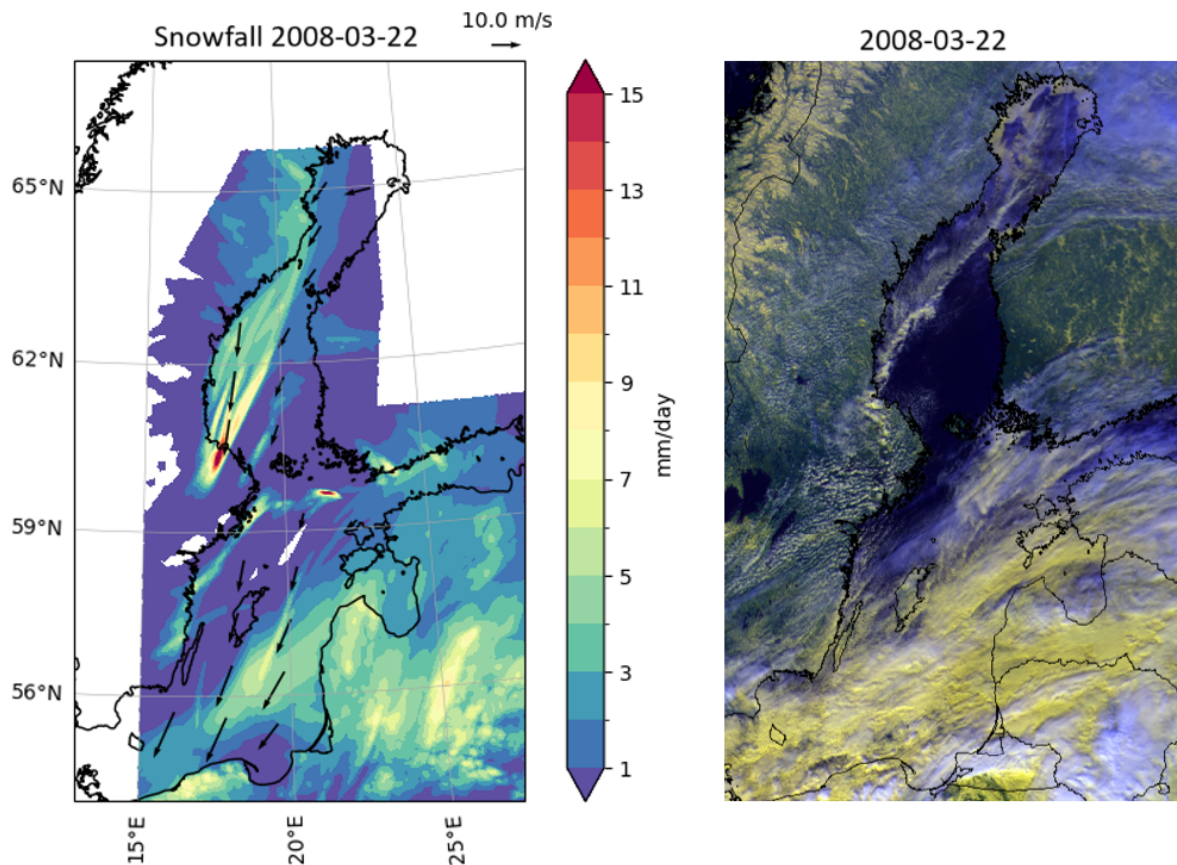


Figure 1: HCLIM-simulation of snowfall (mm/day) with arrows illustrating wind speed and direction, left, and a satellite image, right, of the Baltic sea region on 2008-03-22. White elements in the image are clouds, dark blue areas are water, land areas are seen in green, the black lines illustrate land borders and the distinct narrow white band in Sea of Bothnia is a convective snowband. Satellite image received by personal communication from SMHI, June 2024.

In addition to the temperature gradient, wind is an important factor in the formation of convective snowbands. With a strong wind and low directional wind shear, meaning a small change in wind direction with height, the convective cells will become organized into cloud streets. Wind speeds influence the type of bands that are formed where higher wind speed have been linked to higher precipitation rates (Olsson et al. 2020). Niziol (1987) discussed that higher directional shear can lead to (i) singular greater bands splitting into several weaker ones, (ii) bands spreading out and reducing in strength and (iii), in cases of severe shear, cause the band structure to fall apart altogether or prevent them from forming in the first place. Well organized bands are typically found when directional shear is less than 30° through the so called 'steering layer' (surface up to the 700 hPa level), although convective snowbands can form with a shear of up to 60° . Together the wind speed and direction determine the flow path and therefore the place of impact as well as the fetch of the air mass, meaning how far it travels over open water. A longer fetch implies a greater moisture input to the overlying air resulting in more precipitation (Jeworrek et al. 2017).

The resulting snowfall in these events is influenced by convection depth and moisture input, where heavier snowfall has been related to deeper convection (Braham 1983 see Rothrock 1969). The convection depth, and therefore cloud depth, is usually limited by the height of the atmospheric boundary layer (ABL) and its enclosed capping inversion. The ABL can be de-

defined as the part of the troposphere which is affected by the surface of the Earth, both in terms of frictional drag and heat fluxes. Its height can vary from a few tens of meters to several kilometers depending on the meteorological conditions and is confined at the top by a temperature inversion, a stable part of the atmosphere where the temperature increases with height (Stull 2017). However, instability and strong vertical movements can also lead to growth of the ABL. For sufficient convection in terms of snowbands a boundary layer height of minimum 1000 m is usually needed (Braham 1983).

Snowband formation and snowfall amounts can also be affected by other physical features such as the shape of the coast, convergence and topography. Holroyd (1971) showed that both thermal and frictional convergence could impact and enhance the formation of convective snowbands. Frictional convergence results in the air mass over land deflecting to the left in the Northern Hemisphere. If the coast is on the right hand side of the wind direction this then lead to convergence over the water and enhanced vertical movements. Andersson & Gustafsson (1993) and Andersson & Nilsson (1990) also investigated the role of topography and the shape of the coast in snowband formation and found that elongated bays, such as the Gulf of Finland and to some extent the Bay of Bothnia are favourable areas of formation. Additionally, Mazon et al. (2015) found that land breeze circulations (due to thermal differences between land and sea) lead to mid-bay convergence, forcing air to rise, and thereby contribute to the formation of snowbands over the Gulf of Finland.

2.1.2 Recent studies

Predicting sea-effect snowfall accurately is challenging due to the small-scale nature of the events, being formed and maintained by local convective processes. Historically, forecasting of these events has been difficult but over the years this has greatly improved, primarily due to advancement in models and methods for weather forecasts along with growing observational networks, both in situ and remote sensing (Fujisaki-Manome et al. 2022). For example, a case study by Jungfeldt (2020) looked at the performance of the high-resolution weather prediction model HARMONIE in simulating a selection of convective snowband events over the Baltic area and coastal Sweden, showing that intense snowbands are captured very well, with a slight overestimation in precipitation, however, future studies of weaker bands are needed. Other recent studies of sea-effect snowfall in the Baltic region (e.g. Jeworrek et al. 2017; Olsson et al. 2020; Olsson et al. 2023) have shown that identifying these events using regional climate models is possible and can be done for longer time series to study the climatology of the phenomena. These articles established threshold values for favourable meteorological conditions regarding snowband formation that were then applied on model data for identification of events in the Baltic sea region. The set of conditions were based on previous research and process studies, as discussed above, and were adapted to the region of interest by studying known cases along the Swedish and Finnish coasts. Jeworrek et al. (2017) also investigated different model configurations such as horizontal grid resolution of 0.22° , 0.16° and 0.11° (corresponding to approximately 25, 16 and 12.5 km) and found that increasing the resolution in a RCM as well as a coupling of the RCM to a high-resolution ocean model lead to better representation of convective snowbands.

2.2 Numerical weather and climate models

Models are simplified ways to describe the real world and can be used to gain knowledge of a system and its underlying processes or, for example, make predictions of future system response. Often used in the context of meteorology and climate are numerical model systems based on mathematical equations describing physical processes in the atmosphere, land and oceans and since many of these equations are non-linear they are approximated and solved numerically, rather than analytically (Stull 2017). Numerical Weather Prediction (NWP) models, used to produce short term weather forecasts (usually up to 2 weeks), and climate models simulating several decades describing long term averages and variability of weather, apply equations from thermodynamics and fluid mechanics to simulate the weather for discrete time steps. To do this the Earth is divided into a grid of stacked 3D boxes covering the entire surface and reaching into the atmosphere. The grid boxes have a certain horizontal resolution in degrees of longitude and latitude or meters, as well as a vertical resolution depending on the number of vertical levels chosen, related to height and atmospheric pressure. Gridpoints are assigned attributes describing the topography needed to calculate the meteorological, hydrological and oceanographical conditions in that box (SMHI 2023a). Processes that occur on smaller scales than the grid resolution (so called sub-grid processes), for example cloud formation and radiation processes, need to be treated in so called parameterizations, which describe these processes in a simplified way through semi-empirical and statistical relations. These can differ between models but also in the configurations of the same model since higher resolution allows certain processes to be resolved to a greater extent. The final product constitutes complex models often requiring large computational resources to run (Rummukainen 2010).

Global climate models (GCMs) simulate the entire atmosphere on the planet and due to the large area and limited computational resources a coarse grid is needed, typically $O(100 \text{ km})$. Regional climate models (RCMs) are run over a limited regional domain enabling higher resolution, usually $O(10 \text{ km})$. Since the RCMs only simulate a designated part of the globe they need input supplied by either GCMs or reanalysis. The latter is in practise hindcasts with a NWP model assimilating observations, aimed at representing the actual past conditions as close as possible. This coarser data is used as boundary conditions to the RCM, fed into the model at the edges of its domain and often at sea-surface, unless the RCM is coupled with an ocean model. This method is called dynamical downscaling (Rummukainen 2010). Often a system of nested RCMs of different grid sizes are used to step-wise increase resolution over progressively smaller domains. Mainly due to increasing computational power, RCMs are becoming increasingly applied at $O(1 \text{ km})$ resolutions. These models are usually referred to as convection-permitting since they use non-hydrostatic dynamics and start to resolve deep convective processes. This leads to potential improvements in the simulation of precipitation, especially short-duration convective precipitation (Schär et al. 2020). The added benefits of a finer grid are therefore a more realistic representation of physical processes and surface features. This does come at a price with more output data leading to long processing times and storage issues (Schär et al. 2020). Another aspect to take into account is that the RCMs inherit biases from their boundary data. Inaccurate forcing data will further propagate in the RCM and lead to poor simulations regardless of the RCM performance (Rummukainen 2010).

With today's RCMs reaching into the single kilometer scale resolution it opens up the interest to study convective snowbands once more. Also, since most previous studies in the Baltic sea area have focused on the historic or present-day climate, thus creating a clear incentive to assess the possible effect of climate change on this phenomena.

3 Data and method

In this project simulations from a RCM with two different grid sizes have been used to first identify convective snowband events and then analyse the frequency, precipitation and meteorological conditions of these events in a historical and future warmer climate.

3.1 Model description and data

This project has utilized simulations from the HARMONIE-Climate (HCLIM) regional climate model framework. The model is based on the related HARMONIE (*HIRLAM-ALADIN Regional Mesoscale Operational NWP in Europe*) NWP modelling system and has been developed as a collaboration between several European meteorological institutes: AEMET (Spain), DMI (Denmark), FMI (Finland), KNMI (the Netherlands), MET Norway and SMHI (Sweden). The HCLIM model system has three configurations: ALADIN, ALARO and AROME, each developed to be applied at different grid resolutions (Belušić et al. 2020). Output data from two configurations of HCLIM have been used here: ALADIN with a horizontal grid resolution of 12 x 12 km, and AROME with a higher resolution, in this case 3 x 3 km, where ALADIN provides boundary data to the AROME simulations. Both configurations use 65 vertical levels. They also employ the same surface model as well as parameterization of radiation, but differ in most other physical schemes e.g. simulation of clouds and turbulence. The biggest difference is that AROME runs at convection-permitting resolutions using non-hydrostatic dynamics and resolves the deep convection, whereas ALADIN uses a convection parameterization. This also enables AROME to advect convective precipitation to nearby gridpoints. Both configurations and the full model system are further described in Belušić et al. (2020) and model performance in e.g. Lind et al. (2020); Lind et al. (2023). The HCLIM ALADIN and AROME configurations are henceforth referred to as HCLIM12 and HCLIM3, relating to the respective horizontal resolution used.

Simulations with two system versions of HCLIM, referred to as cycles, have been assessed: i) Cycle 38 with simulations at both 12 km and 3 km spatial resolution, to investigate the impact of higher model resolution, and available for a historical period forced by the ERA-Interim reanalysis (Dee et al. 2011); and ii) Cycle 43, the latest version, used to study the climate change impact on convective snowbands. Here only 12 km resolution simulations are available for a historic and two future time periods, mid and end of the 21st century. The cycle 43 simulations applied forcing from the ERA5 reanalysis (Hersbach et al. 2018) and a small ensemble of four GCMs from the Coupled Model Intercomparison Project phase 6 (CMIP6), see boundary data and exact time periods in table 1.

All simulations of future time periods are based on a relatively high emission scenario called Shared Socioeconomic Pathway 3-7.0 (SSP370). This scenario represent a future with slow technical advancement, growing nationalism and conflict, where global issues, such as climate change, are not prioritised. The scenario leads to an end of century radiative forcing of 7.0 W/m² and a global mean temperature rise of about 4 °C compared to pre-industrial times (IPCC 2023). Simulations for SSP127, a "greener" scenario compatible with the 2.0 °C target, were also available, however, since this project aims to study the phenomena in a future warmer climate SSP370 was opted for.

Table 1: Model configurations and boundary data used.

HCLIM version	Grid resolution	Boundary data	Time period
cycle 38	3 km & 12 km	ERA-Interim (reanalysis)	1998-2018
cycle 43	12 km	ERA5 (reanalysis) & GCMs: MPI-ESM, CNRM, MIROC6, EC-Earth	1980-2014 2030-2060 (SSP370) 2070-2100 (SSP370)

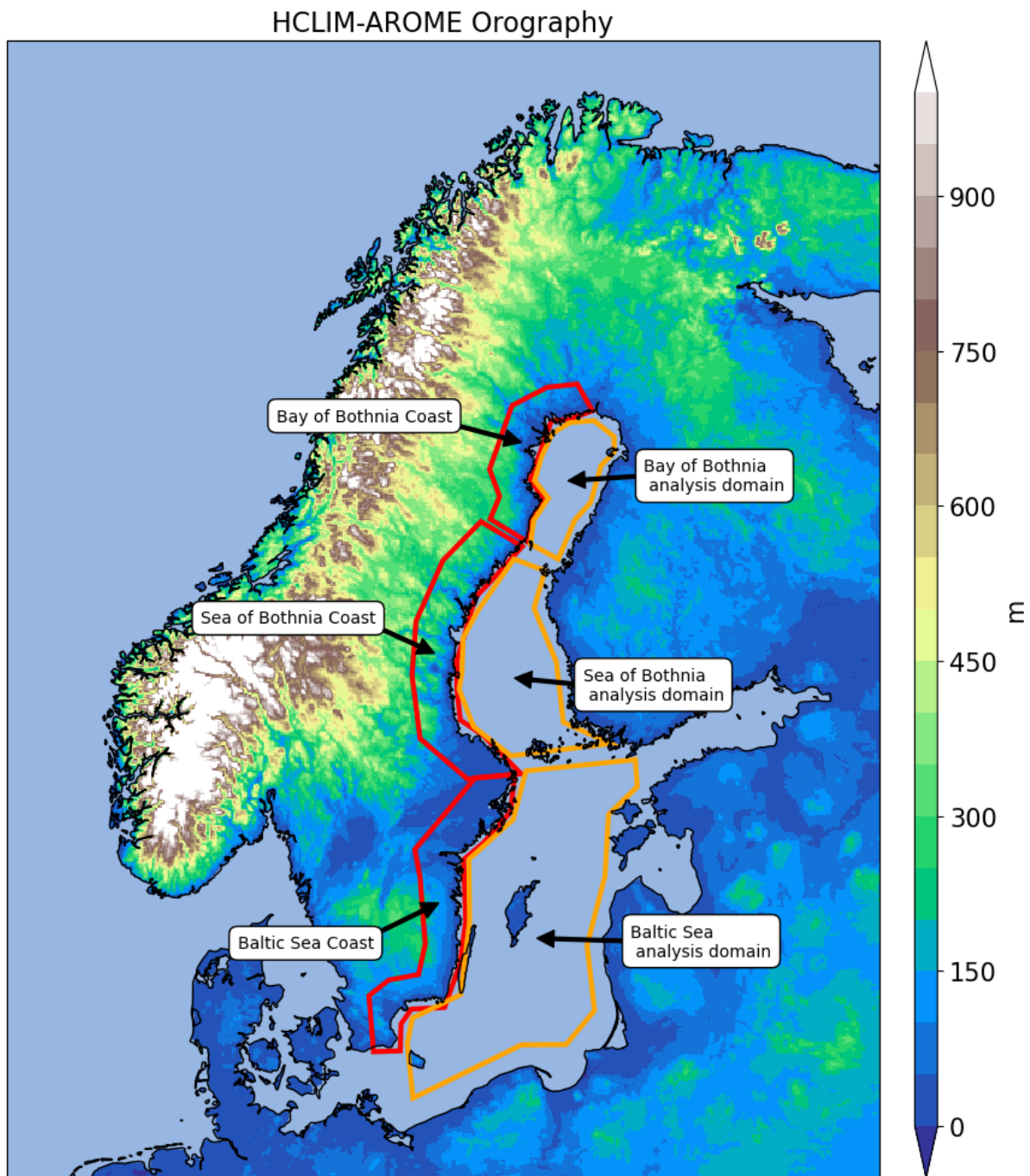


Figure 2: The domain of HCLIM-AROME (HCLIM3) showing the Baltic Sea region with the three analysis areas used, marked in orange, and their corresponding coastal areas, marked in red.

Since convective snowbands are investigated, only data from October to April is used in the analysis, when temperatures are frequently cold enough for snowfall at the surface. The temporal resolution of the analyzed data is 6 hours, providing four data points for each gridbox and day. The resulting data are NetCDF files of meteorological parameters with three dimensions: time, x and y, where x and y are based on degrees of latitude and longitude. For smoother data processing and to enable more area specific statistics the Swedish east coast has been divided into three analysis areas: Baltic Sea, Sea of Bothnia and Bay of Bothnia, further divided into sea and coastal regions (Figure 2).

3.2 Validation data

To evaluate model results and the impact of model grid resolution on simulated precipitation reference datasets of daily accumulated precipitation for the analysed time period 1998-2018 were used. Observations of precipitation are associated with uncertainties, related to instrument errors and uncertainties, limitations in spatial coverage and in post-processing (e.g. interpolation and quality checks) (e.g. Baker et al. 2012). Therefore, two different reference datasets have been used here, see Table 2.

Table 2: Precipitation products used.

Product	Data source	Coverage	Resolution	Frequency	Source
GridClim	SMHI Gridded Climatology, a reanalysis dataset using interpolated observations from weather stations and first guesses by the downscaled UERRA-HARMONIE.	Nordic countries, land and sea	2.5 km	Daily	SMHI (2021)
NGCD	Nordic Gridded Climate Dataset based purely on spatial interpolation of measured precipitation from weather stations.	Finland, Norway, Sweden, land only	1 km	Daily	Copernicus Climate Change Service (2021)

3.3 Methodology

3.3.1 Detection of snowband days

The methodology for identifying convective snowbands is based on Jeworrek et al. (2017) and Olsson et al. (2020) and consists of, for each gridpoint and each time step (6 h), checking that the atmospheric conditions and SST crosses specific thresholds that have been identified as favourable for snowband formation. Then in the same gridpoint also check that precipitation and snowfall occurred to "confirm" that convection took place and lead to snowfall. The choice to verify precipitation directly in place with the other criteria for each gridpoint, rather than as a second step for a larger area of interest like Jeworrek et al. (2017), was made to try and minimise other type of precipitation in vicinity causing falsely identified snowband events.

The thresholds used in this project are presented in Table 3 and are primarily based on Jeworrek et al. (2017) "weak criteria" for the Swedish Baltic sea area, but have been adjusted due to

recent research and model differences. The weak criteria were chosen since a test run showed that the strong criteria (including e.g. a larger temperature gradient and higher wind speeds) excluded many less intense snowband events while here the aim is to identify as many convective snowbands as possible. A day was defined as a snowband day if all of these criteria were fulfilled in at least one gridpoint in one 6 h period that day.

Table 3: Criteria used to detect snowband days. Different output levels were available for the two HCLIM cycles; when different values for pressure levels are given these refer to cycle 38/cycle 43.

Parameter	Criteria
Temperature difference (between SST and air at 850 hPa)	> 13 °C
Sea surface temperature	> 0 °C
Boundary layer height	> 1000 m
Directional wind shear (between 700 and 950/1000 hPa)	< 60°
Wind speed (at 10 m)	> 7 m/s
Wind direction (at 900/925 hPa)	between 350-360°, 0-140°
6h max intensity of total precipitation	> 0.5 mm/h
6h accumulated snowfall (liquid equivalent)	> 0.5 mm/6h

Adjustments compared to Jeworrek et al. (2017):

The wind speed threshold has been lowered from 10 to 7 m/s since Olsson et al. (2020) case study showed snowband events occurring at these lower wind speeds at the Finnish coast. The 2 m temperature criteria was dropped since snowfall is a criteria and that implies low air temperature. A condition of SST being above zero degrees was added accordingly to Olsson et al. (2020) to confirm that the water surface is ice free. The span of wind direction was extended since Vesslén (2013) showed that events can occur during south-easterly winds as well. Her sensitivity study found that approximately the same amount of events occur for wind directions between 90-120° as 20-40°. Finally the snowfall criteria was adjusted to match the difference in temporal resolution, the threshold of 1.5 mm/day was lowered to 0.5 mm/6h.

3.3.2 Analysis

In this project Python, primarily the Xarray and Numpy packages, were utilized to process the multidimensional data files and perform different analyses.

Frequency of events

Number of snowband days were analysed for each individual gridpoint, each analysis area and for the entire Swedish Baltic sea area. Since the simulated time periods are not all of equal length frequencies were calculated per year rather than in total number of occurrences.

To compute the frequency of events the detection method described in section 3.3.1 was applied to each simulation. The result is a mask where gridpoints and time steps fulfilling all snowband criteria have been set to the value 1, while the others to NaN (Not a Number), effectively blocking the data where the criteria is not met. Since SST and the temperature difference between SST and air at 850 hPa are applied criteria all land areas are by definition masked out. From this mask the frequency of days for each gridpoint can be obtained, resulting in maps of the spatial distribution of snowband days. A time vector of all identified snowband days for a specific area can also be derived.

Favourable days for snowband formation are defined as days when the wind, SST, ABL and temperature difference (SST-T850) fulfill their respective criterion, however, this does not necessarily mean that convective precipitation actually occurred. The number of favourable days as well as days when snowband precipitation reached some part of the Swedish coast were calculated. Snowband precipitation reaching the coast was defined as days when the precipitation and snowfall criteria were fulfilled in at least one gridpoint within the coastal regions (Figure 2).

Meteorological parameters

Analysis of meteorological parameters has been done using both the above mentioned masks, to extract parameter values solely from gridpoints fulfilling all snowband criteria, and the time vector to analyse the whole spatial field (including land points) for specific snowband days. The last method does, however, mix in zeros when analysing precipitation (places where no precipitation occurred) into the statistics unless filtered. Mainly averages, spread and certain percentiles have been calculated and analysed spatially and in general.

Ensemble estimation

When studying climate change it is generally good practice to use several climate models or several realizations with a single climate model (called multi-model or single-model ensemble respectively) since no model is can capture the full complexity perfectly. Different models use different parameterizations and numerical methods resulting in varying performances and biases. Using an ensemble then both provides a more accurate portrayal of the developments and an assessment of the uncertainty in model formulation and impact of initial conditions (Copernicus Climate Change Service n.d.). The ensemble average (HCLIM12-ENS) was calculated by taking the average of the ensemble members (HCLIM12-GCM) individual results, e.g. number of snowband days per year or precipitation for each simulation. The ensemble spread was represented either by the max/min estimate of the ensemble members or by the standard deviation with respect to the ensemble average. To portray the ensemble spread in the spatial maps the sign of change in future predictions (+/-), indicating increase or decrease of a parameter in the future, for each individual ensemble member was used. In gridpoints where at least 75% of the ensemble members, in this case minimum 3 out of 4, project the same sign of change a striped pattern was added. The ensemble results were evaluated for the recent past by comparing with the HCLIM12-ERA5 simulation.

Impact of model resolution

To investigate the impacts and potential benefits of a convection-permitting resolution the frequency of snowband days and meteorological parameters were compared between HCLIM3 and HCLIM12, in simulations forced by ERA-Interim (ERA-Interim) for the 1998-2018 time period. When identifying snowband days for these two simulations the boundary layer criterion was omitted since that parameter was not available as output for HCLIM12 in cycle 38. When identifying snowband days for HCLIM3 the threshold for the number of gridpoints that needed to fulfill all criteria for a day to be classified, was revisited since the threshold of one gridpoint (approximately $3 \text{ km} \times 3 \text{ km} = 9 \text{ km}^2$) did not seem comparable to that of the coarser resolution model ($12 \text{ km} \times 12 \text{ km} = 144 \text{ km}^2$). To match this a lower limit of 16 gridpoints needed to fulfill all criteria to be defined as a snowband day in the HCLIM3 simulation, since this matches the HCLIM12 gridbox area. Snowband days were compared both in totals, since both simulations were of same length (21 years), and per year, this was done spatially and in number of events for each defined analysis area.

Averages and 90th percentiles for daily precipitation (mm/day) for snowband days were calculated for each gridpoint and compared with the reference datasets introduced in section 3.2. Only precipitation from snowband days found in both HCLIM12 and HCLIM3 were used. For visual comparison the datasets were analysed on their respective original grids. When deviations between model results and reference datasets have been calculated the data was first remapped to the coarsest grid using bilinear interpolation. Before the average/percentile was calculated the precipitation time series for each gridpoint were compared statistically using the non-parametric Wilcoxon Rank Sum test, since precipitation is rarely normally distributed. This is used to test whether the snowband precipitation in the model results and the reference datasets were drawn from similar distributions.

4 Results

4.1 Present-day climate

The frequency of snowband days for the historic period 1980-2014 is shown in Figure 3. Areas with higher occurrences along the Swedish coast can be seen around Västerbotten, Gävleborg and northern parts of Uppland, as well as around Öland and the coast of Småland. Many events also occur in the middle of the Baltic sea area, reaching the north of Gotland, but also as far south as the coast of Poland. On the order of 2-3 snowband days per year occur in these areas, while we see about 18-25 days per year in the Baltic sea area, 10-15 days per year in Sea of Bothnia area and about 5-10 days per year in Bay of Bothnia. Numbers are impacted by the size of each analysis area. Within the whole Swedish Baltic Sea region 25-30 snowband days per year were found, often with events occurring in several areas at once.

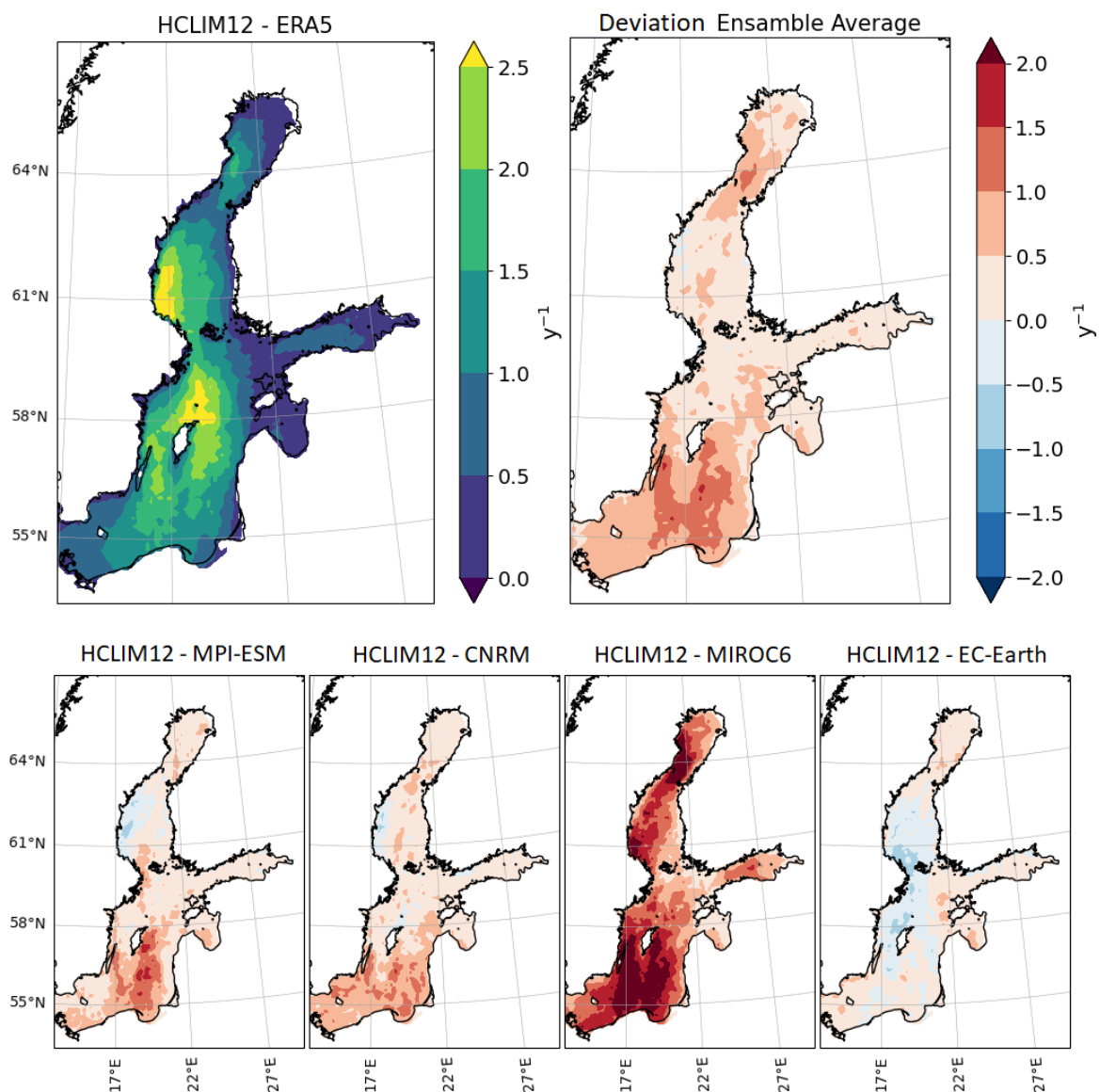


Figure 3: Frequency of snowband days for the historic period, 1980-2014. The total number of days per year for HCLIM12-ERA5, top left, and the ensemble average deviation from HCLIM12-ERA5, top right. The bottom row presenting the deviation in results for each single downscaled GCM with respect to HCLIM12-ERA5. The top right colorbar applies to all deviation plots.

Using HCLIM12 forced by ERA5 as a reference for the present day climate, Figure 3 shows deviations in the ensemble models. From a slight underestimation of events in the HCLIM12-EC-Earth simulation to a large overestimation in the in the HCLIM12-MIROC6 simulation. The resulting ensemble average lead to a general overestimation of events compared to HCLIM12-ERA5. However, the overall difference is low, below 0.5 days per year, with the exception of the southern Baltic Sea and the main impact area in Bay of Bothnia, see Figure 3. The same analysis with HCLIM12-MIROC6 excluded from the ensemble results in smaller deviations, Figure B17 in Appendix.

The overestimation of snowband days is associated with a larger SST-T850 temperature difference simulated in most HCLIM12-GCMs compared to HCLIM12-ERA5. That criterion is therefore fulfilled more often. In the northernmost region, Bay of Bothnia, higher SSTs and lower sea ice cover in the GCMs also have an impact. Monthly averages of SST-T850 and sea ice cover for Bay of Bothnia can be seen in Figure 4, where the HCLIM12-MIROC6 simulation stand out by having the clearly largest biases compared to HCLIM12-ERA5. The same analysis for the Baltic Sea and Sea of Bothnia show continued higher SST-T850 in the ensemble models but with smaller deviations from February and onwards (Figure D24 in Appendix), while for sea-ice two GCMs instead overestimate the ice cover, mainly in Sea of Bothnia but to some extent also in the Baltic Sea (for the Baltic Sea region, sea-ice is primarily confined to the Gulf of Finland). Other criteria and how often they are fulfilled in the GCM downscalings versus ERA5 can be seen in Figure D25 in Appendix.

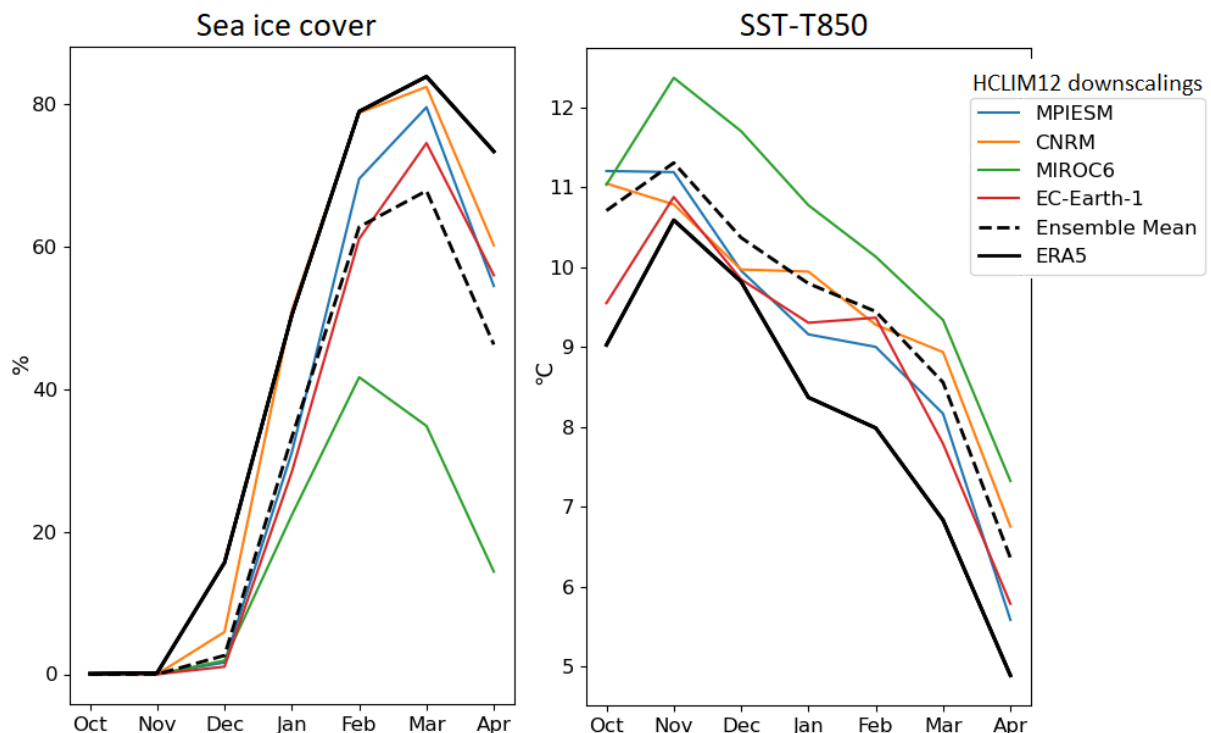


Figure 4: Monthly averages in the Bay of Bothnia analysis domain of sea ice cover, left, and the temperature difference between the sea surface and air at the 850 hPa level, right. Results are shown for all downscaled GCMs (HCLIM12-GCM), the ensemble average and HCLIM12-ERA5 for the historical run, 1980-2014.

Averages of the meteorological conditions during snowband events are shown in Table 4 for HCLIM12-ERA5. The mean boundary layer height and temperature difference during events are on average slightly higher in the Baltic Sea area, while precipitation amounts are seemingly greater in the northern regions. The resulting ensemble average of these are alike that of HCLIM12-ERA5 results (Table D9, D10 and D11 in Appendix).

Windroses indicate that snowband events occur primarily during northerly winds in the Baltic sea area and north to north east winds in the Bay and Sea of Bothnia (Figure 5). Examining wind for more intense events, snowfall > 5 mm/6h, showed an association with higher wind speeds and less dominance of northerly winds. The boundary layer height was also found to be higher on average for these events (2520 m, 2470 m and 2140 m for Baltic Sea, Sea of Bothnia and Bay of Bothnia respectively in HCLIM12-ERA5).

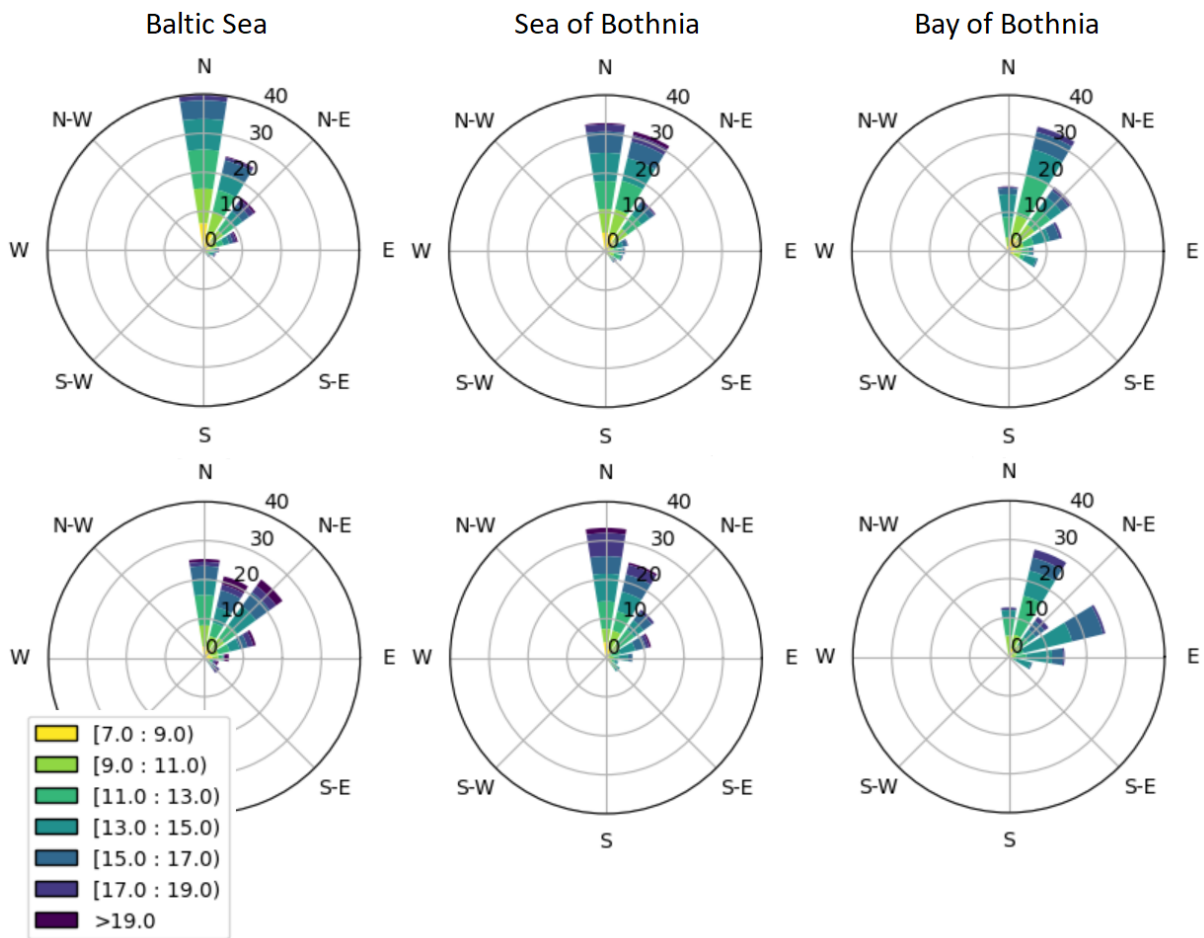


Figure 5: Wind from HCLIM12-ERA5 gridpoints fulfilling all snowband criteria, top row, and an additional criterion: snowfall > 5 mm/6h, bottom row. The legend and colors signify wind speed (m/s). The rings: 0, 10, 20 and 40 indicate % of total occurrences.

Table 4: HCLIM12-ERA5, average and standard deviation in parenthesis of meteorological parameters for gridpoints (6h timesteps) fulfilling all snowband criteria. Precipitation and snowfall were also resampled to daily accumulated amounts.

Parameter	Baltic Sea	Sea of Bothnia	Bay of Bothnia	Criteria
ABL Height (m)	2170 (690)	2040 (650)	1860 (620)	> 1000
SST (°C)	4.3 (2.2)	3.8 (1.9)	4.6 (1.6)	> 0
TempDiff (°C)	17.1 (2.6)	16.7 (2.2)	16.6 (2.3)	> 13
Directional wind shear (°)	19.8 (15.0)	20.8 (15.6)	23.1 (15.7)	< 60
Wind speed (m/s)	12.1 (3.1)	12.3 (2.9)	12.2 (2.6)	> 7
Precipitation (mm/6h)	2.5 (1.4)	2.7 (1.5)	3.1 (1.6)	
Precipitation (mm/day)	5.4 (3.6)	5.8 (4.0)	6.9 (4.1)	
Snowfall (mm/6h)	2.1 (1.3)	2.4 (1.4)	2.7 (1.5)	> 0.5
Snowfall (mm/day)	4.3 (3.1)	5.0 (3.5)	6.0 (3.8)	

The spatial distribution and average snowfall rates for all identified snowband days in the Swedish Baltic Sea region is shown in Figure 6. The spatial pattern matches the main impact areas identified in Figure 3 for snowband frequencies. Ensemble results also correspond well to that of the downscaled reanalysis, though with a slight underestimation in the upper Baltic sea area and Sea of Bothnia (particularly close to the Swedish coast), while the opposite is seen for the Bay of Bothnia region. Deviations are small, rarely larger than ± 0.2 mm/day or $\pm 15\%$.

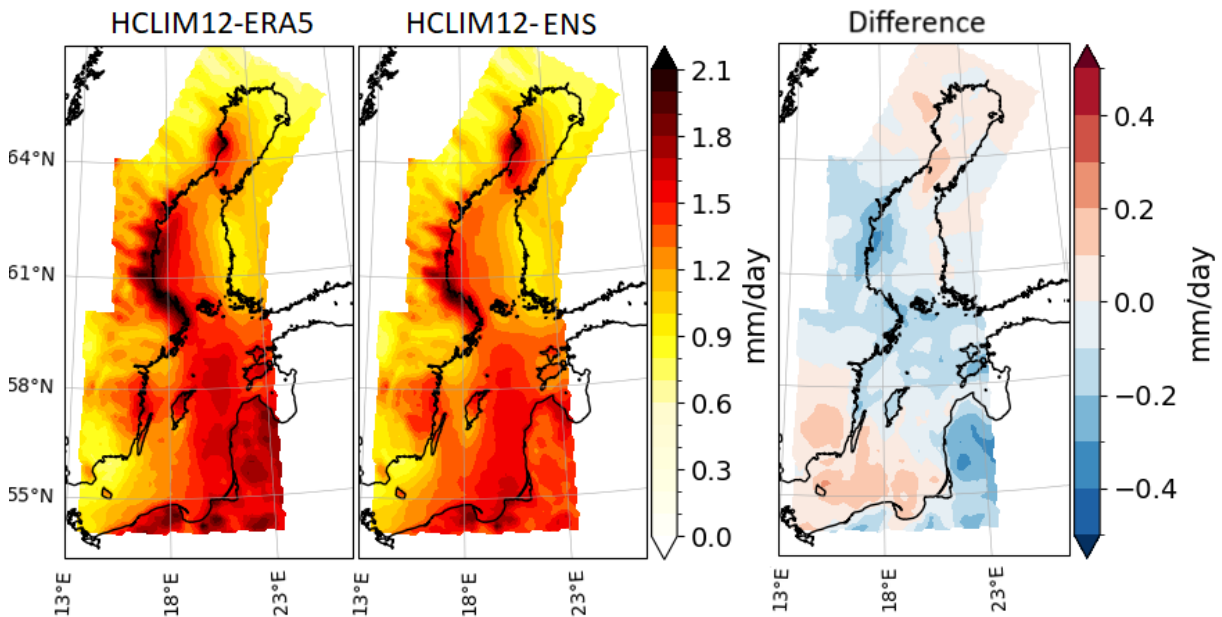


Figure 6: HCLIM12-ERA5, the ensemble average, HCLIM12-ENS, and the ensemble deviation from HCLIM12-ERA5 in snowfall (mm/day) for all snowband days in the Swedish Baltic Sea region. Historic period 1980-2014.

The ensemble average of median, mean and 75th percentile of snowband precipitation is shown in Figure 7. Studying each analysis area separately once again shows that snowfall and precipitation rates are higher further north. The snow fraction of total precipitation is also lower over water and in southern regions. The precipitation presented in these two figures (6, 7) are unfiltered, meaning precipitation values for the entire field have been chosen for each snowband

day even though the snowband impacts a very small located area, zeros are then mixed into the averages for the places not impacted. The result is lower than actual snowband intensities in the graphs, more accurate averages are displayed above (Table 4), with snowfall rates of 4-6 mm/day depending on the region.

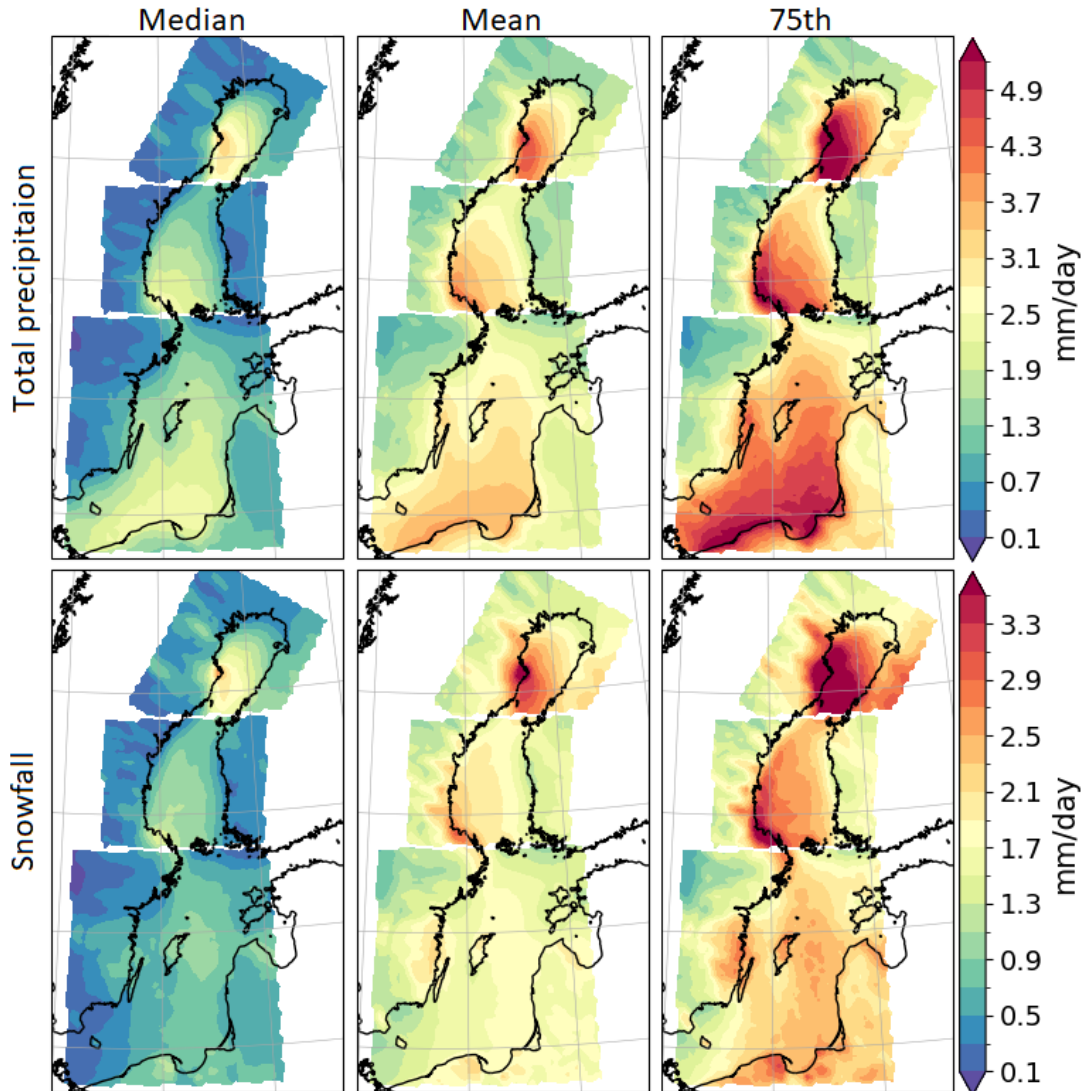


Figure 7: The Ensemble average of median, mean and 75th percentile of total precipitation, top row, and snowfall, bottom row, (mm/day) for selected snowband days from each analysis area.

4.1.1 Impact of model resolution

Results from the two HCLIM-ERA-Interim simulations run for 1998-2018 using 3 km and 12 km horizontal grid resolution (HCLIM3 and HCLIM12) vary in both frequency of events and snowband precipitation. The contrast in model resolution, distribution of snowband days and average precipitation can be seen in Figure 8. Both simulations present similar spatial patterns of events, though with lower frequencies in HCLIM12. Overall more snowband days are simulated by HCLIM3, about 31 days per year for the whole Swedish Baltic sea region, while HCLIM12 simulates around 22 days per year, Table 5. The extra days in HCLIM3 primarily occur over the Baltic Sea, with roughly 65% higher frequency compared to HCLIM12, and over the Sea of

Bothnia with an almost 35% higher occurrence of days. In Bay of Bothnia 14% fewer days were identified in HCLIM3 compared to HCLIM12, however, measured in events per year, the difference is low, less than a day. Out of the HCLIM12 identified snowband days only about 58% of the days were found to be identical to that of HCLIM3 days in the Bay of Bothnia region whereas the same number for the other regions lies between 85-90%. The two models simulated similar impact areas for snowband precipitation, although in HCLIM12, the precipitation does not reach as far inland over the coastal regions. In general HCLIM3 produced higher precipitation averages over land and lower over water.

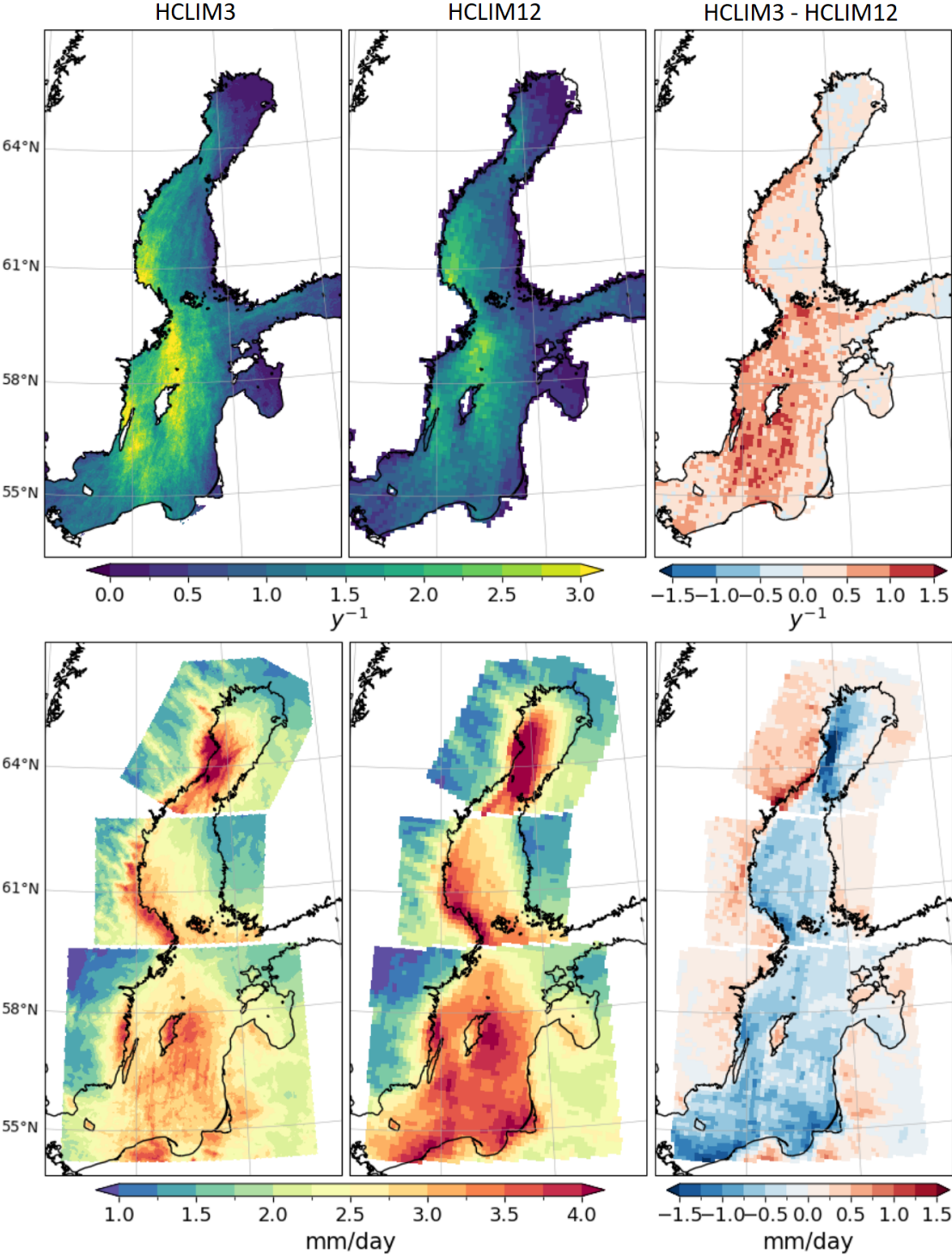


Figure 8: Frequencies of snowband days per year (without ABL criteria), top row, and average snowband precipitation (mm/day), bottom row, for HCLIM3, HCLIM12 and the difference between the two simulations, right. HCLIM3 interpolated to the HCLIM12 grid for calculation of deviation.

Table 5: Number of snowband days in total and per year found in the HCLIM3 and HCLIM12 ERA-Interim 1998-2018 downscaled simulations. Identical refers to the number of days found to be identical in the two simulation results.

Region	HCLIM3		HCLIM12		Identical total
	total	per year	total	per year	
Baltic Sea	535	25.5	322	15.3	293
Sea of Bothnia	313	14.9	232	11.0	195
Bay of Bothnia	102	4.9	119	5.7	69
All areas	645	30.7	453	21.6	412

Distribution and percentiles of total precipitation for gridpoints fulfilling snowband criteria in HCLIM3 and HCLIM12 are shown in Figure 9. HCLIM3 demonstrate higher max intensities (mm/h) and higher extreme values of accumulated precipitation/snowfall (above 90th percentile). HCLIM12 instead produced higher accumulated precipitation rates (mm/6h) on average, Table 6. HCLIM3 simulated snowband precipitation in a wider range of intensities, up to maximum values; snowfall 50.1 mm/6h and precipitation rate of 25 mm/h. The equivalent numbers in HCLIM12 are 15.7 mm/6h and 6.8 mm/h.

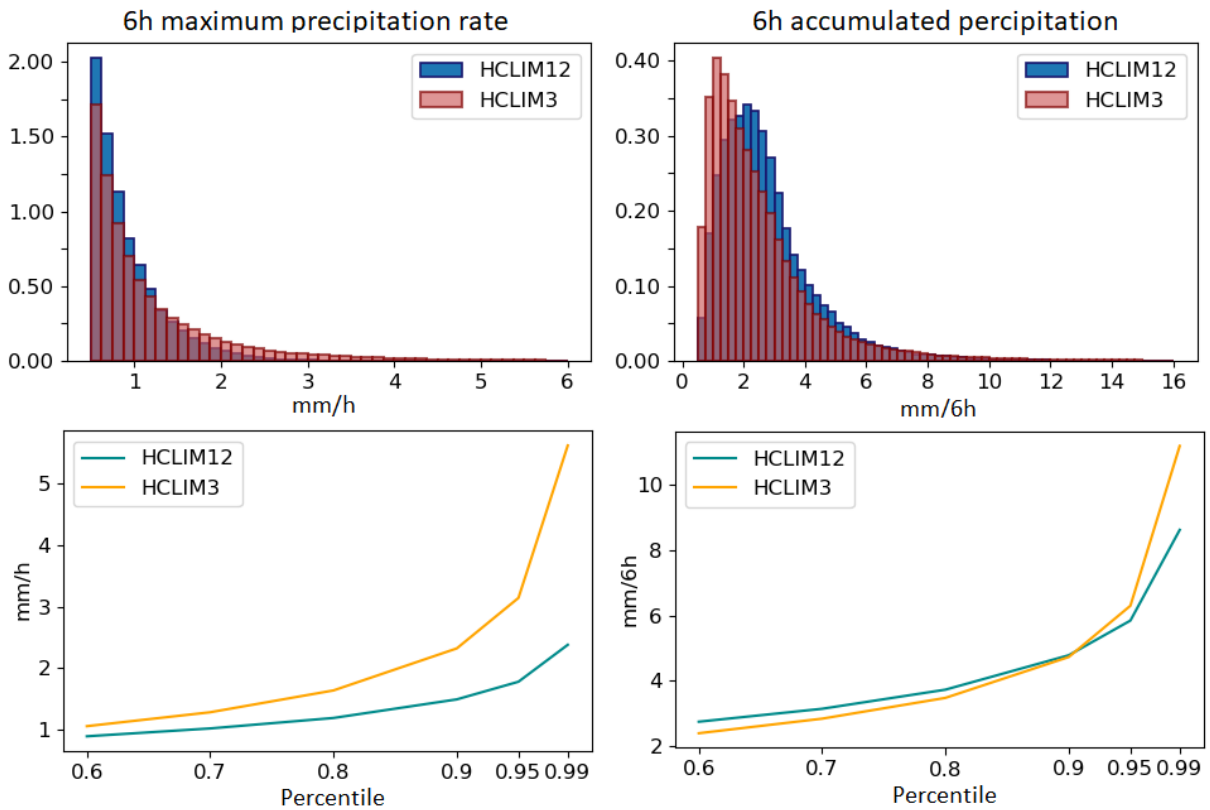


Figure 9: Normalized distribution, top row, and percentiles, bottom row, of both max intensity (mm/h) and accumulated total precipitation (mm/6h) for gridpoints fulfilling snowband criteria.

Table 6: Precipitation for gridpoints fulfilling snowband criteria. Values are presented: HCLIM3 / HCLIM12. When average (avg.) is given the standard deviation is listed in parenthesis. 99th refers to the respective percentile.

Parameter	Baltic Sea	Sea of Bothnia	Bay of Bothnia
Avg. Max precipitation (mm/h)	1.28 (1.11) / 0.93 (0.41)	1.19 (0.94) / 0.91 (0.44)	1.10 (0.87) 0.92 (0.46)
Avg. Precipitation (mm/6h)	2.56 (2.23) / 2.69 (1.59)	2.69 (2.09) / 2.91 (1.59)	2.72 (1.83) / 3.28 (1.95)
Avg. Snowfall (mm/6h)	2.25 (1.81) / 2.30 (1.28)	2.47 (1.86) / 2.62 (1.4)	2.55 (1.72) / 2.73 (1.33)
99th Precipitation (mm/6h)	11.36 / 8.50	10.83 / 8.28	9.83 / 11.11
99th Snowfall (mm/6h)	9.27 / 6.72	9.72 / 7.33	9.21 / 7.5

Comparing precipitation averages of model results with observational products illustrate that both HCLIM3 and HCLIM12 matches the overall spatial patterns but overestimate precipitation over water (Figure 10 and C20 of 90th percentiles in Appendix). In general both models correspond well to that of GridClim over the Swedish east coast as indicated by the Wilcoxon Rank Sum results with a significance level of 5%, suggesting that the simulated precipitation amounts in the models are drawn from the same distribution as of that in the reference dataset. Over water deviations are smaller between HCLIM3 and GridClim than that of HCLIM12 and GridClim, both when comparing averages and area where the precipitation distributions are significantly different.

When comparing to NGCD deviations in average precipitation for snowband days are larger than that the deviation to GridClim for a few localised areas. Overall the simulated precipitation differs significantly (confidence level of 95%) from NGCD for both models for most of the domain, with exception of the coastal hot spot areas on the coast in Bay of Bothnia and Sea of Bothnia and over Gotland. A slightly larger area where the precipitation distributions are not significantly different is seen in the HCLIM12-NGCD comparison.

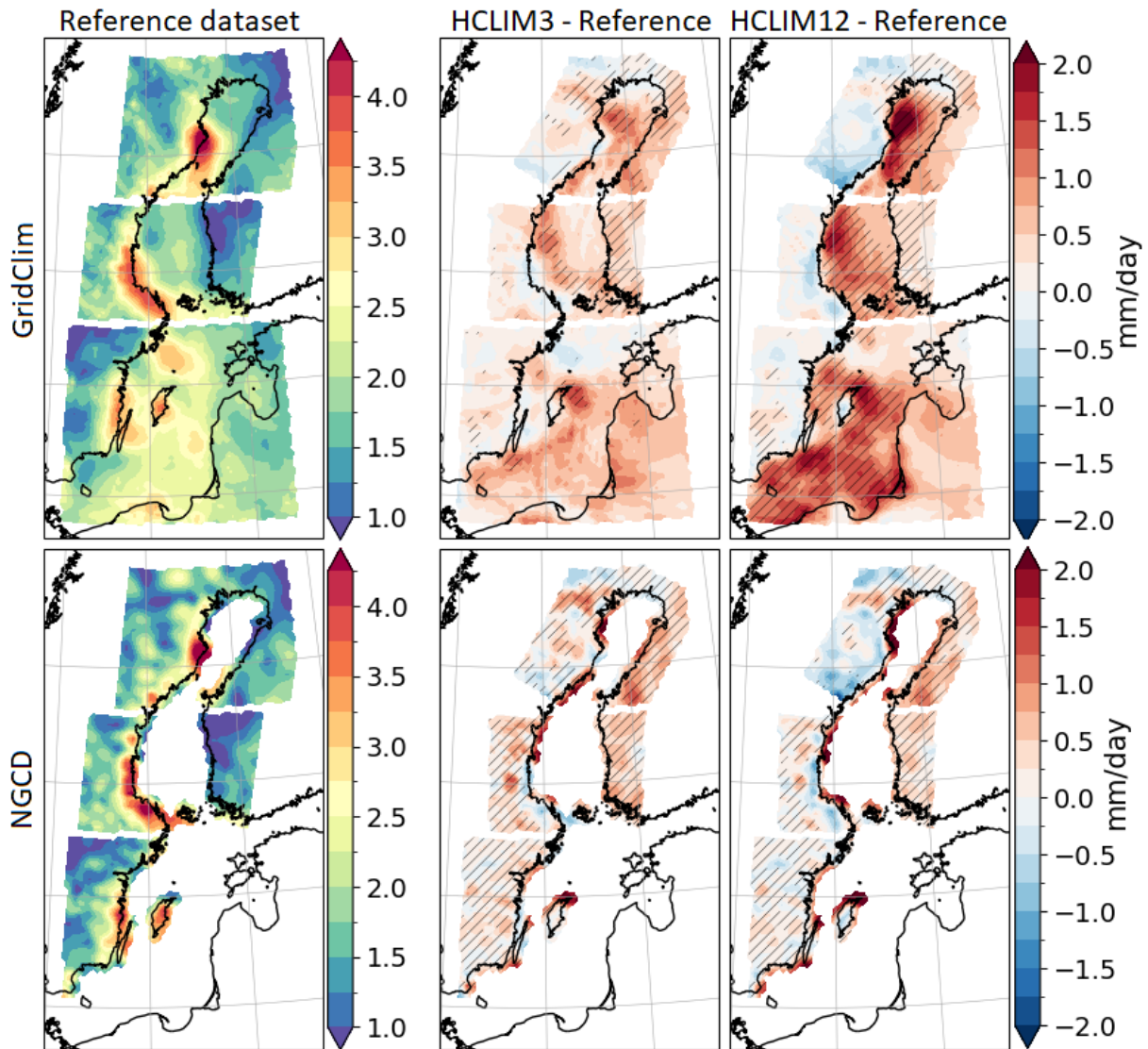


Figure 10: Average precipitation for snowband days identified in both HCLIM3 and HCLIM12. Reference datasets; GridClim, top row, NGCD, bottom row, and the deviation in HCLIM3, HCLIM12 with respect to each reference. All precipitation datasets have been interpolated to the largest grid resolution. Striped pattern indicate areas where the Wilcoxon result is significant ($p\text{-val} < 0.05$) and the precipitation time series in the model vs. obs are not drawn from the same distribution.

4.2 Future projections

Future predictions of convective snowbands demonstrate a likely decrease in number of events along the Swedish east coast, especially towards the end of the century and in the southern parts of the Baltic Sea, Figure 11. A slight increase can be seen in a few local places, e.g. in areas usually ice covered in the later winter months in present day climate (see Figure D26 in Appendix). However, the total number of events per year for each analysis area all decrease towards both mid and end of the century, see Figure 12 and Table 7.

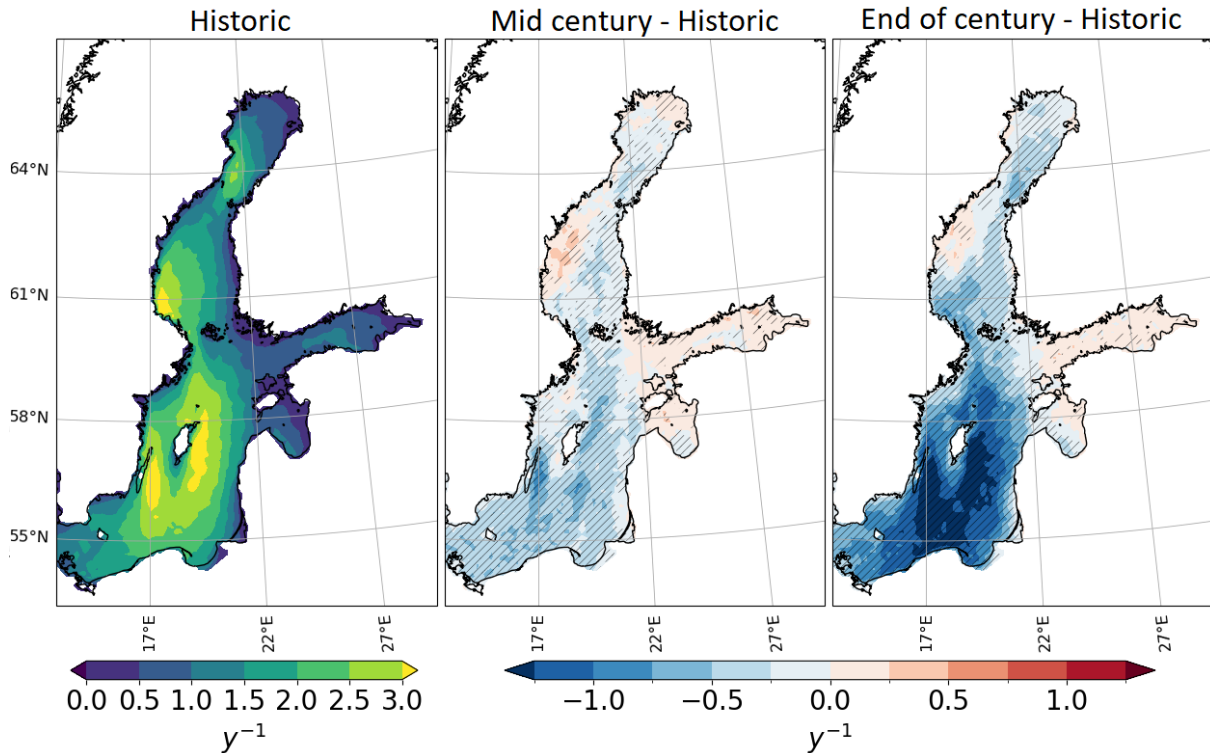


Figure 11: Ensemble average of frequency of snowband days per year. Historically, 1980-2014, and projected changes towards mid (2030-2060) and end (2070-2100) of the century. The striped pattern indicate areas where at least 75% of the ensemble models exhibit same sign in the projected change (+/-).

The seasonal cycle demonstrates a peak of snowband occurrences in Nov-Dec in Bay of Bothnia and Sea of Bothnia, and in Dec-Jan in the Baltic Sea in historic simulations, Figure 12. In the future scenarios the total number of events per year decreases on the whole and the frequency peak shifts forward in the season; to Dec-Jan in the north and Jan-Feb in the Baltic Sea. A future warmer climate might also lead to an extended snowband season in Bay of Bothnia, primarily due to reduced sea-ice cover in the future. Change in ice cover is shown in Figure D27 in Appendix for each ensemble model. This pattern of seasonal shift is more clear in Figure B19 in Appendix where the HCLIM12-MIROC6 has been disregarded from the ensemble results.

The results also show that the number of favourable days for snowband formation might slightly decrease in the Baltic sea and increase in the northern regions in the future, Table 7. Though the share of favourable days leading to convective snowbands reduces, meaning factors not taken into account in the criteria for favourable days are limiting snowband formation. A probable one is air temperature affecting whether precipitation falls in solid or liquid form. This is further confirmed when analysing number of snowbands days per year with the snowfall criterion neglected: these instead shows an increase of events in the future, see Figure A15 in Appendix. Additionally, the share of snowband days where snowfall reaches the Swedish coastline differs between analysis areas. This ratio is around 90 % in Sea of Bothnia and closer to 70-75 % in Bay of Bothnia and the Baltic Sea in the historic simulation. Furthermore the percentage of events reaching the coast seem to increase in the future simulations for all areas, Table 7. See also Table A16 in Appendix for individual model results as well as the ensemble average of future change, rather than total number of events (as in Table 7), which shows a smaller ensemble spread. The favourable days, snowband days and coast days from HCLIM12-ERA5 and

ensemble results disregarding HCLIM12-MIROC6 can also be seen in Table B8 in Appendix, indicating less deviation from HCLIM12-ERA5.

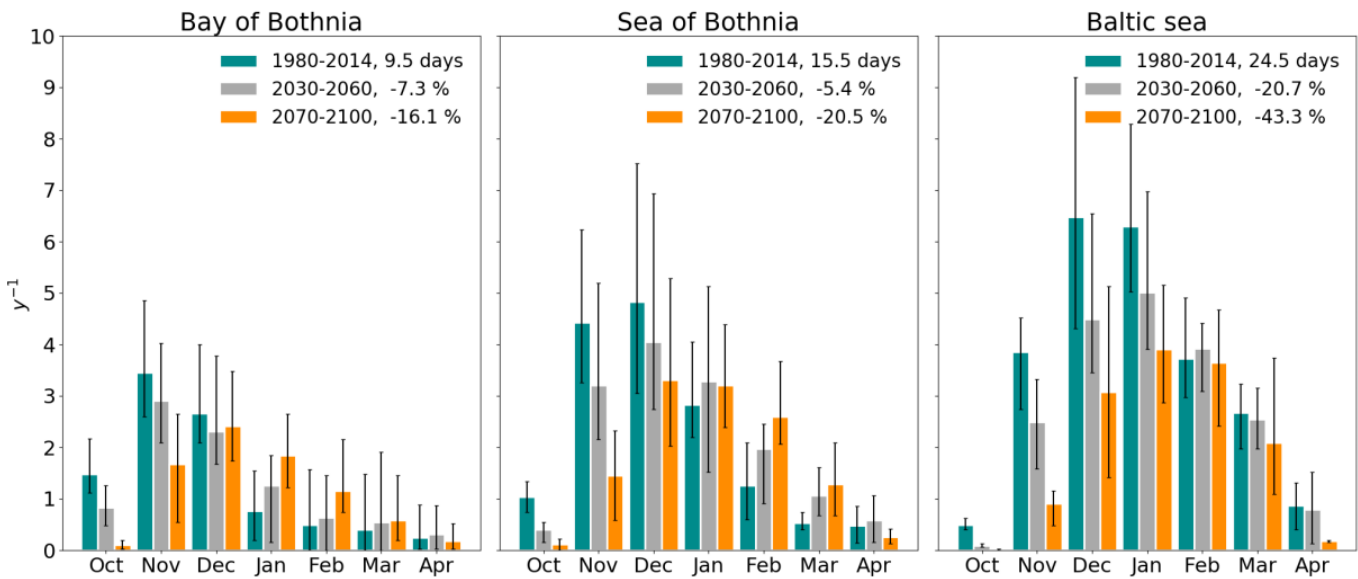


Figure 12: Ensemble average of number of snowband days per year and month. Errorbars showing the maximum and minimum value of the ensemble. Legend showing the total number of days per year and the future change.

Table 7: Ensemble average and standard deviation in parenthesis of total number of days per year. Favourable days for snowband formation, confirmed snowband days and days where snowbands reached the Swedish coast. The percentage indicate the share of favourable days where snowfall occurred and the share of snowband days where snowfall occurred over the coast.

Region	Time period	Favourable	Snowband	%	Coast	%
Baltic Sea	1980-2014	64.4 (9.6)	24.4 (5.6)	37.9	18.0 (4.6)	73.7
	2030-2060	63.6 (10.1)	19.4 (4.5)	30.4	14.7 (3.8)	76.2
	2070-2100	61.7 (13.0)	13.8 (4.6)	22.4	10.9 (3.8)	78.7
Sea of Bothnia	1980-2014	44.2 (9.0)	15.4 (4.6)	34.9	13.8 (4.3)	89.8
	2030-2060	46.6 (10.1)	14.6 (5.5)	31.3	13.1 (5.1)	90.0
	2070-2100	46.3 (11.5)	12.2 (4.4)	26.4	11.1 (3.8)	90.5
Bay of Bothnia	1980-2014	31.3 (7.7)	9.5 (4.0)	30.4	6.6 (3.0)	69.7
	2030-2060	33.8 (9.7)	8.8 (3.9)	26.1	6.3 (2.9)	71.7
	2070-2100	35.8 (9.6)	8.0 (3.4)	22.3	6.0 (2.8)	75.0
All areas	1980-2014	78.2 (12.2)	33.2 (7.9)	42.5	27.2 (7.1)	81.8
	2030-2060	78.6 (12.8)	28.2 (7.6)	35.9	23.6 (6.6)	83.6
	2070-2100	76.9 (16.3)	21.9 (7.3)	28.4	18.7 (6.4)	85.7

Future projections show increasing total precipitation for snowband days over nearly the entire Swedish Baltic Sea region towards the end of the century, with emphasis on the main impact areas, Figure 13. The relative increase is highest over land in the Bay and Sea of Bothnia regions, Figure C21 in Appendix. A similar pattern can be seen for snowfall amounts over land in the two northern regions. The southernmost part of the Swedish coast does, however, not illustrate any change in the median and mean values towards the end of the century compared to the

historic period (less than ± 0.1 mm/day), while there is a small increase in the 75th percentile value over the coast of Småland. Overall, the mid century projections show the same change patterns but with a smaller magnitude, with exception of the Baltic Sea coast where snowfall rates increase more, Figure C23.

Over water snowfall rates show a decline in future scenarios, especially towards the end of the century. Reductions of more than 60% are seen in the southern parts of the Baltic sea, whereas reductions north of Gotland are mostly less than 30%, Figure C22. This pattern of increasing snowfall amounts over land and decreasing over the water is possibly an effect of the increasing air temperatures, Figure D28 in Appendix. For selected snowband days the mean air temperature increases over the ocean areas to near or above zero degrees Celsius, while still staying well below zero over land. This might cause precipitation to more frequently reach the surface as rain over the water but still as snow over land.

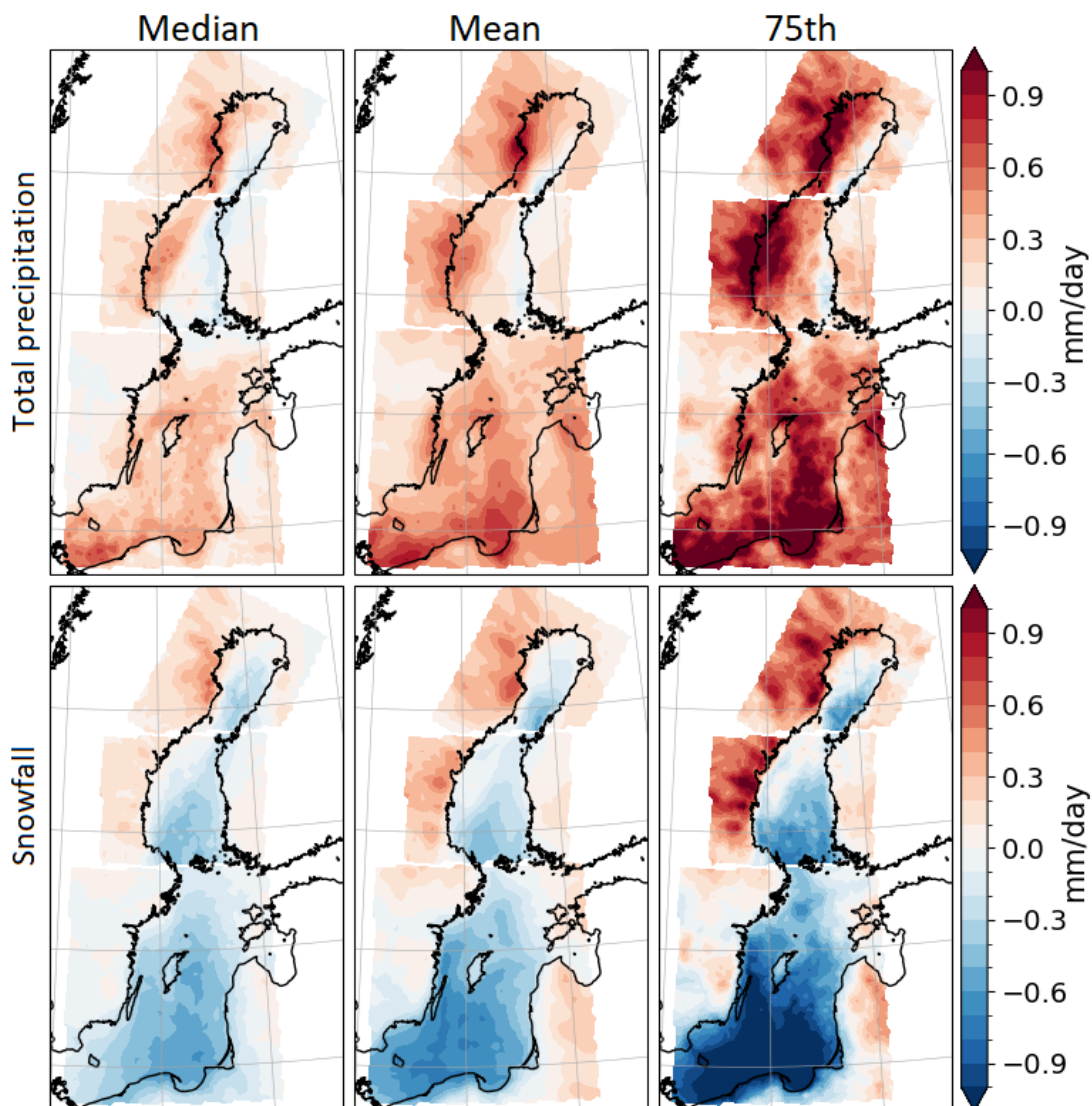


Figure 13: Change in the ensemble average of median, mean and 75th percentile of total precipitation, top row, and snowfall, bottom row, towards the end of the century for selected snowband days. Here end of century (2070-2100) – historic (1990-2014).

Analyzing the frequency of events where the snowfall rates are more intense, > 10, 20 mm/day, over the coastal regions shows that out of all days where snowband precipitation occurs over land around 25% of these are above 10 mm/day and about 4% above 20 mm/day in the Baltic Sea area, Figure 14. In Bay of Bothnia and Sea of Bothnia the corresponding numbers are around 37% and 8%. While the total number of snowband occurrences decreases in the future scenarios, the HCLIM12-ENS average of percentage of days with intense snowfall rates increases (although with small magnitude compared to the ensemble spread) over the Sea of Bothnia and Bay of Bothnia.

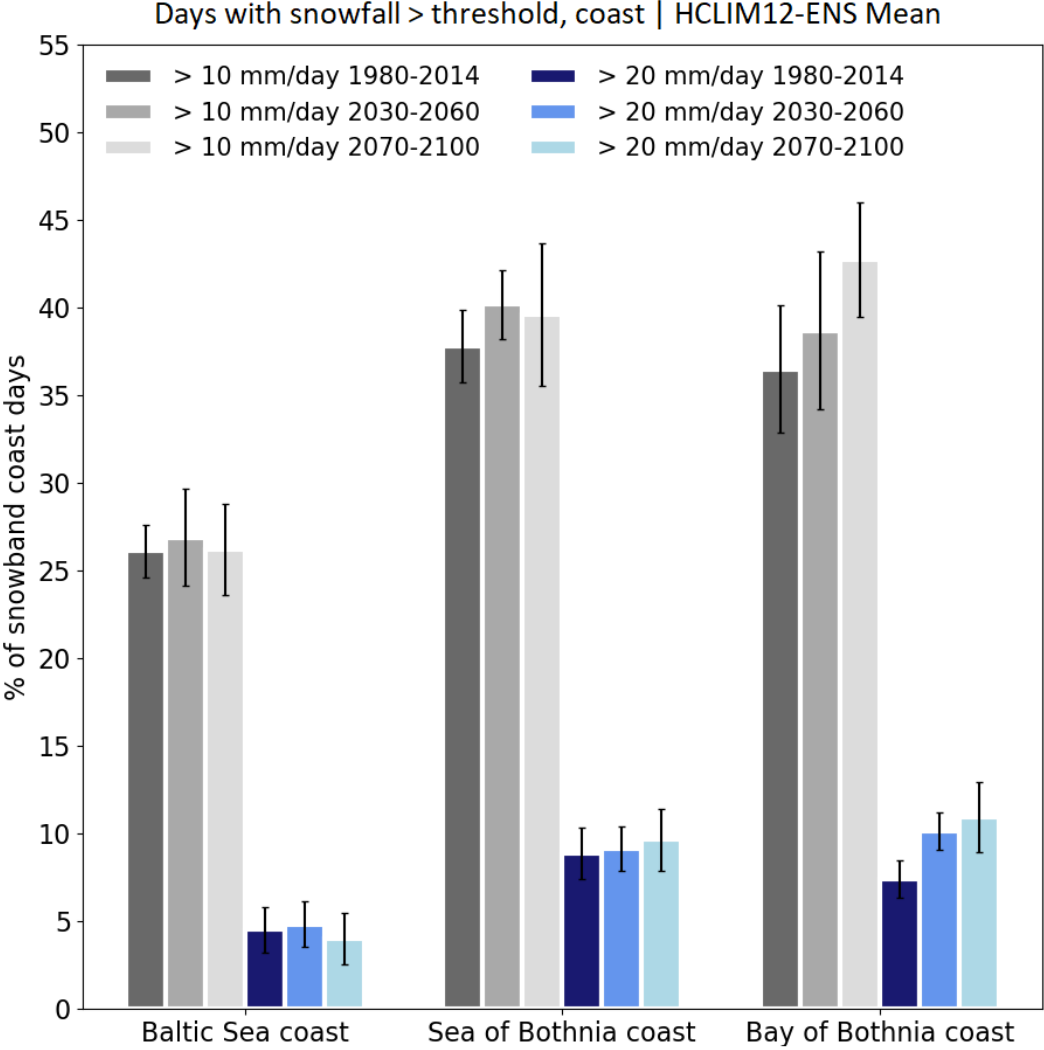


Figure 14: Ensemble average of the share of days with snowfall rates > 10 and 20 mm/day over the coast, calculated for days when snowband precipitation reaches the coast. Errorbars showing the standard deviation of the ensemble.

5 Discussion

5.1 Present-day climate

When analysing the frequency of snowband days there are deviations between the ensemble results and the ERA5 downscaling, as seen by the overestimation in number of days. Said overestimation seems to mainly be caused by higher SSTs in combination with lower temperatures in the overlying air simulated by the GCMs which propagate further in the HCLIM downscaling. This leads to a steep vertical temperature gradient which was seen to be both larger on average and its related criteria was fulfilled more often in certain places and ensemble models, with emphasis on the HCLIM12-MIROC6 simulation. The boundary layer height criteria was also fulfilled more often in areas showing overestimation, in part, possibly due to the unstable conditions more frequently simulated. Despite this, the spatial patterns of main impact areas of convective snowbands in the ensemble results are similar to that of HCLIM-ERA5 which adds credibility to the analysis presented here. A larger disagreement is seen when comparing total number of snowband days for individual areas, especially in Bay of Bothnia where the ensemble average shows a 60% higher frequency of days. The Bay of Bothnia does overall seem like a challenging area to simulate. Here all models, even HCLIM12-EC-Earth which in other areas is in good agreement with HCLIM12-ERA5, struggle with overestimation and differ in recurrence of meteorological conditions favourable for snowband formation (figure D25 in appendix). The ensemble models have higher frequencies of favourable wind direction and higher SST-T850. The struggle to simulate accurate sea ice cover is likely a main cause as well, since ice drastically decrease the fluxes of moisture and heat between air and sea.

It is also clear that the ensemble does perform better when disregarding the HCLIM12-MIROC6 results in terms of frequency of events. Since the MIROC6 simulation effectively bumps up the ensemble average by sometimes simulating up to twice as many events as other ensemble members in the same area. The ensemble deviations from the reference are more than halved without the MIROC6 simulation and the ensemble spread is reduced greatly. With knowledge of these biases one might opt against using MIROC6 or rather using a weighted ensemble average when analysing the Baltic Sea area in the future.

Two previous studies of the same sort; Jeworrek et al. (2017) and Dieterich et al. (2020), both using the same snowband criteria and the same RCM with ≈ 25 km horizontal resolution, have resulted in around 10 snowband days per year for the entire Swedish Baltic sea region. The corresponding number in this project is roughly 26 (HCLIM12-ERA5). This larger value is likely a combination of more generous wind criteria, a higher model resolution as well as a slightly different detection method used in the analysis. In their studies favourable snowband conditions have been checked over the whole Baltic Sea while the precipitation and snowfall over a region covering both land and parts of the sea along the Swedish east coast. This method might be more prone to disregard events in the eastern Baltic Sea directed towards Poland and the Baltic countries, decreasing the number of snowband days found in the Baltic Sea area.

The studied snowband precipitation shows a characteristic spatial pattern corresponding to the areas of higher occurrences showed in frequency of events (Figure 6). A similar pattern of main impact areas also seen in Jeworrek et al. (2017), although with lower snowfall rates found over water and in the Bay of Bothnia area. Snowfall amounts in the ensemble are in good agreement with those seen in HCLIM12-ERA5, which adds credibility to the ensemble estimations.

The meteorological conditions for the selected snowband days are similar for the ensemble results and the ERA5 simulation, with the exception of, on average, higher SSTs and SST-T850 in the ensemble snowband events. The occurrence of certain conditions are however not alike HCLIM12-ERA5, leading to the overestimation in days discussed above. Meteorological conditions and snowfall rates also correspond to those found in snowband cases by Jeworrek et al. (2017) and Olsson et al. (2023), expected since similar criteria were used for detection. The HCLIM-simulations did however produce higher boundary layer heights (around 20% higher than Jeworrek et al. (2017) and 50% higher than Olsson et al. (2023)) and higher wind speeds on average. The average snowfall rate was found to be 4.3-6.0 mm/day, depending on region, where Jeworrek et al. (2017) found an average of 5.8 mm/day overall. That study did, however, apply more restrictive snowfall criteria of > 1.5 mm/day, compared to, essentially > 0.5 mm/day here, though checked over 6h time steps. Masking out snowfall below the higher threshold might increase the average snowfall found in this project.

In line with previous studies by e.g. Braham (1983) and Olsson et al. (2023) results also showed stronger wind and greater boundary layer height, therefore greater possible convection depth, for snowband events with higher snowfall rates (> 5 mm/6h). On the whole the wind analysis showed few cases with wind speeds lower than 9 m/s and with wind direction $> 90^\circ$ meaning the more generous wind criteria used in this study might not have been essential.

5.2 Impact of model resolution

Results from the two different model resolutions show that a higher resolution, convection-permitting, model simulated more snowband events in general. This is true when looking at all days from the entire Swedish Baltic Sea region as a whole, as well as from each individual analysis area, with exception of Bay of Bothnia. What differs in the simulations over the Bay of Bothnia region needs to be further investigated to understand why the higher resolution model simulated fewer events and why the models simulated snowbands on different days to a larger extent while using the same forcing.

Analysing differences in the precipitation produced in the two models indicates that HCLIM3 showed tendencies to simulate more intensities linked to convective precipitation events, which are often short but intense. Results also demonstrate that HCLIM3 can capture the very high precipitation rates that can occur during e.g. extreme snowband events, simulating snowfall rates up to 50 mm/6h where the HCLIM12 maximum value was nearly 16 mm/6h. However, whether these tendencies actually mean higher performance and more realistic modelling of convective snowbands needs further studying. When comparing the model results to different reference datasets no clear answer was found. HCLIM3 shows better performance when comparing results to GridClim, however this might be expected since GridClim is a reanalysis product using the related NWP model on which HCLIM3 is based on. NGCD is based purely on interpolation of measured precipitation which makes it highly dependent on station placement and unfortunately not covering sea areas where the two models deviate the most in simulated precipitation, both compared to each other and to GridClim. Overall, finding a reference dataset of good quality, coverage, high resolution also "non-biased" towards either model to prove difficult since non exist today. Such datasets are necessary to evaluate the high-resolution models representation of this type of local and intensive phenomena and one should should strive to develop it. To answer which model configuration simulates convective snowbands more accu-

rately requires a more in-depth analysis of the precipitation intensities simulated and possibly calculate spatial correlation between precipitation maps rather than compare these visually.

5.3 Future projections

Analysing the future projections shows that a decrease in frequencies of snowband events is anticipated over the entire Swedish Baltic Sea region in a future warmer climate. This contrasts with the hypothesis mentioned in the introduction that warmer SSTs and more frequent ice free conditions could lead to more sea-effect snowfall in the future. This reduction in occurrence is, of course, influenced by a number of things but the main cause seem to be higher air and sea surface temperatures leading to fewer days with solid precipitation, similar results were also found by Dieterich et al. (2020). Though as seen when performing the same analysis without snowfall criteria we will likely see more convective precipitation events overall, hinting at an increase of intense local rainfall along the coast during the winter season. The uncertainties (given by the ensemble spread) in the future projections are larger in the mid century period than the end of century, as well as in the northern regions and in areas usually ice covered in later part of winter (Gulf of Finland and Bay of Bothnia). In these instances there is a bigger spread in the ensemble models, some projecting increases and some decreases, the resulting change is often close to zero. This is possibly due to the large differences in sea ice extent, which discussed above has huge impact on convective events. In the ensemble there is spread both in the sea ice cover in the historical period and in the climate change signal. HCLIM12 forced by MPIESM and MIROC6 simulates an almost complete disappearance of sea ice already in the mid century simulations, while HCLIM12 forced by CNRM and EC-Earth exhibits the same signal only at the end of the century (Figure D27 Appendix).

As seen in table 7 the standard deviation in the ensemble average of snowband days is larger than the future reduction of days, for all but the Baltic Sea area, which question the reliability of the results. However, individually all ensemble models exhibit the same response of decreasing number of events towards the end of century.

The seasonality of convective snowbands demonstrate a forward shift of the peak in occurrences into the later winter months in future projections. Possibly due to warmer temperatures reaching further in to the early winter months preventing snowbands from forming, in combination with less sea ice in the later winter months enabling more events then, though the driving force behind this has not been studied in this project. A similar shift was identified by Olsson et al. (2023) when studying the climatology of convective snowbands in Finland. In October and to a large extent in November, as well as in December over the Baltic Sea area, there are large reductions of events towards the end of the century. The total number of snowband days decrease over the whole season but the results do show increasing number of events occurring in January, February and to some extent March in the two northern regions in future scenarios, as was also found by Dieterich et al. (2020).

Despite the overall decrease in snowband occurrences, future projections show higher total precipitation rates in general during snowband days, in line with other research of climate change in the Baltic Sea area (e.g. Christensen & Kjellström 2018). Whether future snowfall in these events will be more or less intense than in present day climate is harder to ascertain. Snowfall will likely decrease over water, probably due to warmer sea surface temperatures during the winter season, which in turn heat the surrounding air and result in precipitation falling in liquid rather than solid form. Over land things are more complicated, the average snowfall rates

are higher, however, as the share of snowbands reaching the Swedish coast seem to increase as well, it raises the question of what is the leading cause of the increased snowfall averages. When analysing the occurrences of more intense snowband precipitation over the coast (snowfall rates > 10, 20 mm/day), taking the increasing number of days where snowband precipitation reaches the coast into account, the ensemble average stay about same in the Baltic Sea and increase in the northern regions. Hinting at a higher share of intense snowfall events up north in a future warmer climate, though the spread in the ensemble results are large. A more in depth study of simulated snowband intensities and each intensity contribution to the total precipitation is needed.

6 Conclusion

The aim of this thesis was to investigate how convective snowband events might change in both occurrence and intensity in a future warmer climate in the Swedish Baltic Sea area. As well as analyse the impact of a high resolution, convection-permitting regional climate model in this field.

The key conclusions from this project are that convective snowband events will most likely decrease in a future warmer climate, with greatest reductions seen in the south. In the north, events will decrease in total seen over the whole season, however, for specific months occurrences might increase. Projections towards mid 21st century exhibit a larger spread and therefore uncertainty within the ensemble, than those towards the end of the century. According to the climate models future events will exhibit larger total precipitation rates. Snowfall amounts will likely decrease over water, though, over land the changes more uncertain, some indications of higher snowfall intensities were found in the north.

The convection-permitting regional climate model simulated more convective snowband events overall than that of the courser related model. The model resolution also had impact on precipitation rates where the high resolution model simulated higher short term intensities and extreme precipitation events, both related to convective precipitation. However, compared to available observations and reanalysis (NGCD and GridClim) both model resolutions demonstrated similar performance in the simulation of precipitation for selected snowband days.

7 References

- Andersson, T. & Gustafsson, N. (1993). Coast of Departure and Coast of Arrival: Two Important Concepts for the Formation and Structure of Convective Snowbands over Seas and Lakes. *Monthly Weather Review* 122 (6), pp. 1036–1049. DOI: 10.1175/1520-0493(1994)122<1036:CODACO>2.0.CO;2.
- Andersson, T. & Nilsson, S. (1990). Topographically induced convective snowbands over the Baltic Sea and their precipitation distribution. *Weather and Forecasting* 5 (2), pp. 299–312. DOI: 10.1175/1520-0434(1990)005<0299:TICSOT>2.0.CO;2.
- Baker, B., Rasmussen, R., John, K., Tilden, M., Rodica, N., J., P., Craig, S., & D., Y. (2012). How Well Are We Measuring Snow? The NOAA/FAA/NCAR Winter Precipitation Test Bed. *Bulletin of the American Meteorological Society* 93, pp. 11839–.
- Belušić, D., Vries, H. de, Dobler, A., Landgren, O., Lind, P., Lindstedt, D., Pedersen, R. A., Sánchez-Perrino, J. C., Toivonen, E., Ulft, B. van, Wang, F., Andrae, U., Batrak, Y., Kjellström, E., Lenderink, G., Nikulin, G., Pietikäinen, J.-P., Rodríguez-Camino, E., Samuelsson, P., Meijgaard, E. van, & Wu, M. (2020). HCLIM38: a flexible regional climate model applicable for different climate zones from coarse to convection-permitting scales. *Geoscientific Model Development* 13 (3), pp. 1311–1333. DOI: 10.5194/gmd-13-1311-202.
- Braham, R. R. (1983). The Midwest Snow Storm of 8–11 December 1977. *Monthly Weather Review* 111 (2), pp. 253–272. DOI: 10.1175/1520-0493(1983)111<0253:TMSSOD>2.0.CO;2.
- Christensen, O. B. & Kjellström, E. (2018). Projections for temperature, precipitation, wind, and snow in the Baltic Sea region until 2100. *Oxford Research Encyclopedia of Climate Science*. DOI: 10.1093/acrefore/9780190228620.013.695.
- Copernicus Climate Change Service (2021). *Nordic gridded temperature and precipitation data from 1971 to present derived from in-situ observations*. available: <https://www.gloh2o.org/mswep/> [05/20/2024].
- Copernicus Climate Change Service (n.d.). *Why use a model ensemble?* available: <https://climate.copernicus.eu/sites/default/files/2021-01/infosheet6.pdf> [06/15/2024].
- Dee, D. P., Uppala, S. M., Simmons, A. J., Berrisford, P., Poli, P., Kobayashi, S., Andrae, U., Balmaseda, M. A., Balsamo, G., Bauer, P., Bechtold, P., Beljaars, A. C. M., Berg, L. van de, Bidlot, J., Bormann, N., Delsol, C., Dragani, R., Fuentes, M., Geer, A. J., Haimberger, L., Healy, S. B., Hersbach, H., Hólm, E. V., Isaksen, L., Kållberg, P., Köhler, M., Matricardi, M., McNally, A. P., Monge-Sanz, B. M., Morcrette, J.-J., Park, B.-K., Peubey, C., Rosnay, P. de, Tavolato, C., Thépaut, J.-N., & Vitart, F. (2011). The ERA-Interim reanalysis: configuration and performance of the data assimilation system. *Quarterly Journal of the Royal Meteorological Society* 137.656, pp. 553–597. DOI: 10.1002/qj.828.
- Dieterich, C., Gröger, M., Klehmet, K., Berg, P., Jeworrek, J., Jylhä, K., Kjellström, E., Meier, H. E. M., Olsson, T., Wu, L., & Rutgersson, A. (2020). Convective snow bands over the Baltic Sea in an ensemble of regional climate scenarios. *3rd Baltic Earth Conference, Earth system changes and Baltic Sea coasts Conference Proceedings Held Online*, 2-3 June, pp. 63–64. available: https://www.researchgate.net/profile/Zuzanna-Borawska/publication/341827458_Benthic_fauna_influence_on_the_marine_silicon_cycle_in_the_coastal_zones_of_the_southern_Baltic_Sea/links/5ed6444a92851c9c5e726d40/Benthic-fauna-influence-on-the-marine-silicon-cycle-in-the-coastal-zones-of-the-southern-Baltic-Sea.pdf [04/12/2024].
- Fujisaki-Manome, A., Wright, D. M., Mann, G. E., Anderson, E. J., Chu, P., Jablonowski, C., & Benjamin, S. G. (2022). Forecasting lake-/sea-effect snowstorms, advancement, and challenges. *Wiley Interdisciplinary Reviews: Water* 9 (4). DOI: 10.1002/wat2.1594.
- Hedman, L. (1999). *Snökaoset runt Gävle*. Meddelande 151. Stockholm: Styrelsen för Psykologiskt Försvar SPF (Today MSB, The Swedish Civil Contingencies Agency).
- Hersbach, H., P. d. R., Bell, B., Schepers, D., Simmons, A., Soci, C., Abdalla, S., Balmaseda, M. A., Balsamo, G., Bechtold, P., Berrisford, P., Bidlot, J., Boisséson, E. de, Bonavita, M., Browne, P., Buizza, R., Dahlgren, P., Dee, D., Dragani, R., Diamantakis, M., Flemming, J., Forbes, R., Geer, A., Haiden, T., Hólm, E., Haimberger, L., Hogan, R., Horányi, A., Janisková, M., Laloyaux, P., Lopez, P., Muñoz-Sabater, J., Peubey, C., Radu, R., Richardson, D., Thépaut, J.-N., Vitart, F., Yang, X., Zsótér, E., & Zuo, H. (2018). *Operational global reanalysis: progress, future directions and synergies with NWP*.
- Holroyd, E. W. (1971). Lake-Effect Cloud Bands as Seen From Weather Satellites. *Journal of the Atmospheric Sciences* 28 (7), pp. 1165–1170. DOI: 10.1175/1520-0469(1971)028<1165:LECBAS>2.0.CO;2.
- IPCC (2023). *Climate Change 2023: Synthesis Report*. Contribution of Working Groups I, II and III to the Sixth Assessment Report of the Intergovernmental Panel on Climate Change [Core Writing Team, H. Lee and J. Romero (eds.)]. IPCC. Geneva, Switzerland. DOI: 10.59327/IPCC/AR6-9789291691647.

- Jeworrek, J., Wu, L., Dieterich, C., & Rutgersson, A. (2017). Characteristics of convective snow bands along the Swedish east coast. *Earth System Dynamics* 8.1, pp. 163–175. DOI: 10.5194/esd-8-163-2017.
- Jungefeldt, L. (2020). *A Case Study Evaluating the Performance of the NWP Model HARMONIE in Simulating Convective Snow Bands* Uppsala university. Department of Earth Sciences, 2020:12.
- Lind, P., Belušić, D., Christensen, O. B., Dobler, A., Kjellström, E., Landgren, O., Lindstedt, D., Matte, D., Pedersen, R. A., Toivonen, E., & Wang, F. (2020). Benefits and added value of convection-permitting climate modeling over Fenno-Scandinavia. *Climate Dynamics* 55, pp. 1893–1912. DOI: 10.1007/s00382-020-05359-3.
- Lind, P., Belušić, D., Médus, E., Dobler, A., Pedersen, R. A., Wang, F., Matte, D., Kjellström, E., Landgren, O., Lindstedt, D., Christensen, O. B., & Christensen, J. H. (2023). Climate change information over Fenno-Scandinavia produced with a convection-permitting climate model. *Climate Dynamics* 61, pp. 519–541. DOI: 10.1007/s00382-022-06589-3.
- Mazon, J., Niemelä, S., Pino, D., Savijärvi, H., & Vihma, T. (2015). Snow bands over the Gulf of Finland in wintertime. *Tellus A: Dynamic Meteorology and Oceanography* 67 (1). DOI: 10.3402/tellusa.v67.25102.
- MSB (2022). *Handbok i kommunal krisberedskap – 4. Riskkatalog – Stora snömängder*. No: MSB2021 - september 2022. MSB, The Swedish Civil Contingencies Agency. **available:** <https://rib.msb.se/Filer/pdf/30126.pdf>.
- Niziol, T. A. (1987). Operational Forecasting of Lake effect snowfall in Western and Central New York. *Weather and Forecasting* 2 (4), pp. 310–321. DOI: 10.1175/1520-0434(1987)002<0310:OFOLES>2.0.CO;2.
- Olsson, T., Luomaranta, A., Jylhä, K., Jeworrek, J., Perttula, T., Dieterich, C., Wu, L., Rutgersson, A., & Mäkelä, A. (2020). Statistics of sea-effect snowfall along the Finnish coastline based on regional climate model data. *Advances in Science and Research* 17, pp. 87–104. DOI: 10.5194/asr-17-87-2020.
- Olsson, T., Luomaranta, A., Nyman, H., & Jylhä, K. (2023). Climatology of sea-effect snow in Finland. *International Journal of Climatology* 43.1, pp. 650–667. DOI: 10.1002/joc.7801.
- Rummukainen, M. (2010). State-of-the-art with regional climate models. *Wiley Interdisciplinary Reviews: Climate Change* 1, pp. 82–96. DOI: 10.1002/wcc.8.
- Schär, C., Fuhrer, O., Arteaga, A., Ban, N., Charpilloz, C., Girolamo, S. D., Hentgen, L., Hoefler, T., Lapillonne, X., Leutwyler, D., Osterried, K., Panosetti, D., Rüdüsühli, S., Schlemmer, L., Schulthess, T. C., Sprenger, M., Ubbiali, S., & Wernli, H. (2020). Kilometer-Scale Climate Models: Prospects and Challenges. *Bulletin of the American Meteorological Society* 101, E567–E587. DOI: 10.1175/BAMS-D-18-0167.1.
- SMHI (2021). *SMHI Gridded Climatology*. **available:** <https://www.smhi.se/publikationer/publikationer/smhi-gridded-climatology-1.177514> [05/20/2024].
- SMHI (2023a). *Hur fungerar en klimatmodell?* **available:** <https://www.smhi.se/kunskapsbanken/klimat/klimatmodeller-och-scenarier/hur-fungerar-en-klimatmodell-1.470> [05/23/2024].
- SMHI (2023b). *Snökanoner från havet*. **available:** <https://www.smhi.se/kunskapsbanken/meteorologi/sno-och-hagel/snokanoner-fran-havet-1.13740> [03/18/2024].
- Steenburgh, W. J. & Nakai, S. (2020). Perspectives on Sea- and Lake-Effect Precipitation from Japan’s “Gosetsu Chitai”. *Bulletin of the American Meteorological Society* 101 (1), E58–E72. DOI: 10.1175/BAMS-D-18-0335.1.
- Stull, R. (2017). *Practical Meteorology: An Algebra-based Survey of Atmospheric Science*. Vol. Version 1.02b. Vancouver, Canada: University of British Columbia.
- Vesslén, A. (2013). *Kartläggning av snökanoner över Östersjön* Uppsala university. Department of Earth Sciences, 2013:67.

Appendices

A Frequency of events

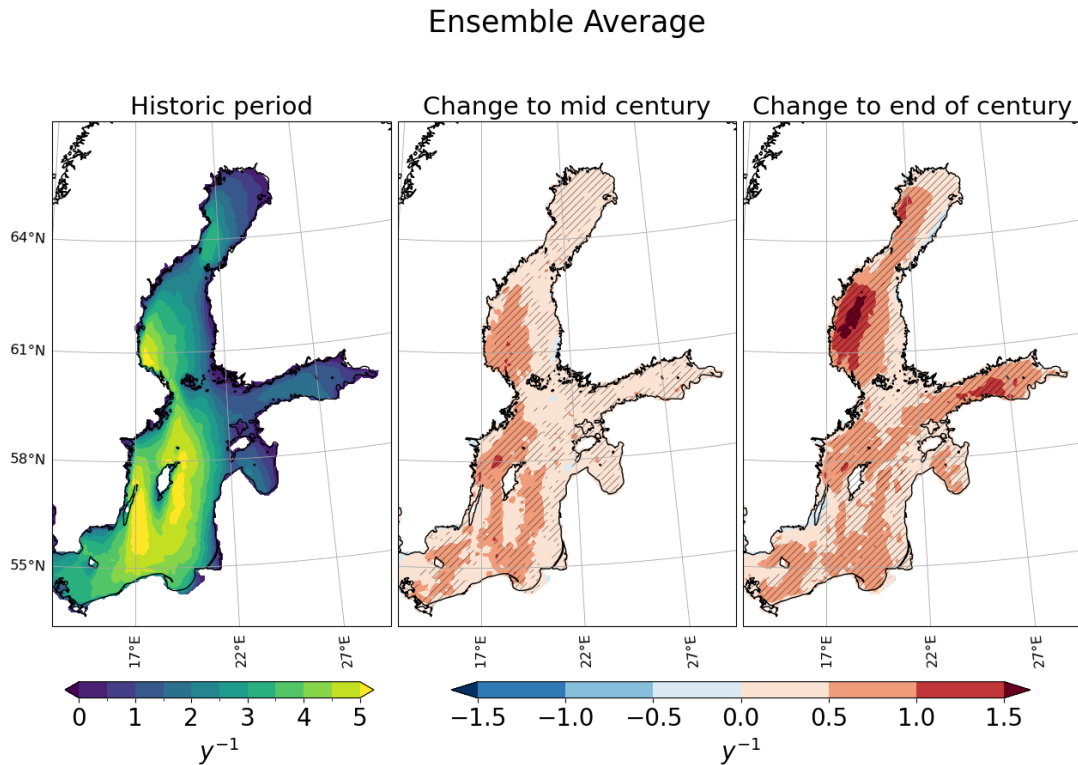


Figure A15: Ensemble average of number of snowband days per year and future change when disregarding the snowfall criterion. Difference here future - historic. The striped pattern indicate areas where at least 75% of the ensemble models exhibit same sign in change (+/-).

Region	Time period	MPIESM	%	CNRM	%	MIROC6	%	EC-Earth	%	Ensemble	%	std
Baltic Sea	1980-2014	24,1		23,5		31,9		18,1		24,4		5,6
	2030-2060	-6,2	-25,9	-6,0	-25,3	-5,9	-18,4	-2,2	-12,0	-5,1	-20,7	1,9
	2070-2100	-8,8	-36,3	-11,2	-47,7	-12,6	-39,6	-9,7	-53,4	-10,6	-43,3	1,7
Sea of Bothnia	1980-2014	13,7		13,3		22,2		12,3		15,4		4,6
	2030-2060	-0,04	-0,3	-2,7	-20,2	0,32	1,4	-0,9	-7,2	-0,8	-5,4	1,3
	2070-2100	-1,6	-11,6	-3,0	-22,6	-3,8	-17,3	-4,2	-33,9	-3,2	-20,5	1,2
Bay of Bothnia	1980-2014	7,8		7,2		15,5		7,6		9,5		4,0
	2030-2060	-0,1	-1,6	-1,4	-19,7	-0,8	-5,5	-0,4	-5,0	-0,7	-7,3	0,6
	2070-2100	-1,2	-14,9	-0,7	-9,4	-2,4	-15,7	-1,9	-24,6	-1,5	-16,1	0,8
Whole coast	1980-2014	31,9		30,7		44,4		25,8		33,2		7,9
	2030-2060	-6,0	-18,8	-6,0	-19,5	-5,0	-11,3	-3,1	-12,0	-5,0	-15,1	1,4
	2070-2100	-9,6	-30,1	-12,2	-39,7	-12,6	-28,4	-11,0	-42,6	-11,4	-34,2	1,4

Figure A16: Number of snowband days historically and change towards the future periods in days per year and percentage for all HCLIM12-GCM simulations. Also showing the ensemble average and standard deviation.

B Ensemble results disregarding HCLIM12-MIROC6

Table B8: Number of days per year estimated in HCLIM-ERA5/HCLIM12-ENS disregarding HCLIM12-MIROC6. Favourable days for snowband formation, confirmed snowband days and days where snowbands reached the Swedish coast.

Region	Favourable	Snowband	Coast
Baltic sea	52.5 / 60.1	19.1 / 21.9	13.7 / 16
Sea of Bothnia	39.1 / 39.7	13.7 / 13.1	12.7 / 11.7
Bay of Bothnia	21.6 / 27.5	5.9 / 7.5	4.2 / 5.1
Whole area	65.4 / 72.5	26.4 / 29.5	21.3 / 23.8

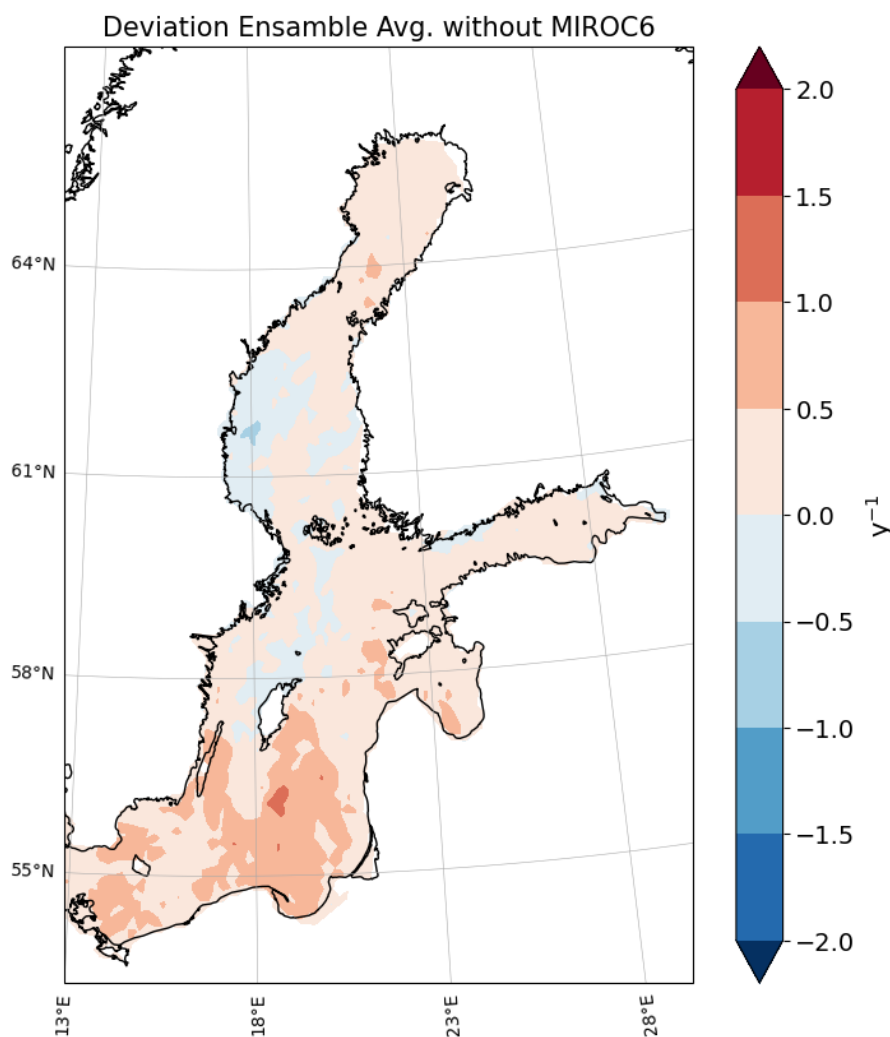


Figure B17: Deviation in number of snowband days per year from HCLIM12-ERA5. Ensemble average without the HCLIM12-MIROC6 simulation, here showing HCLIM12-ENS – HCLIM12-ERA5.

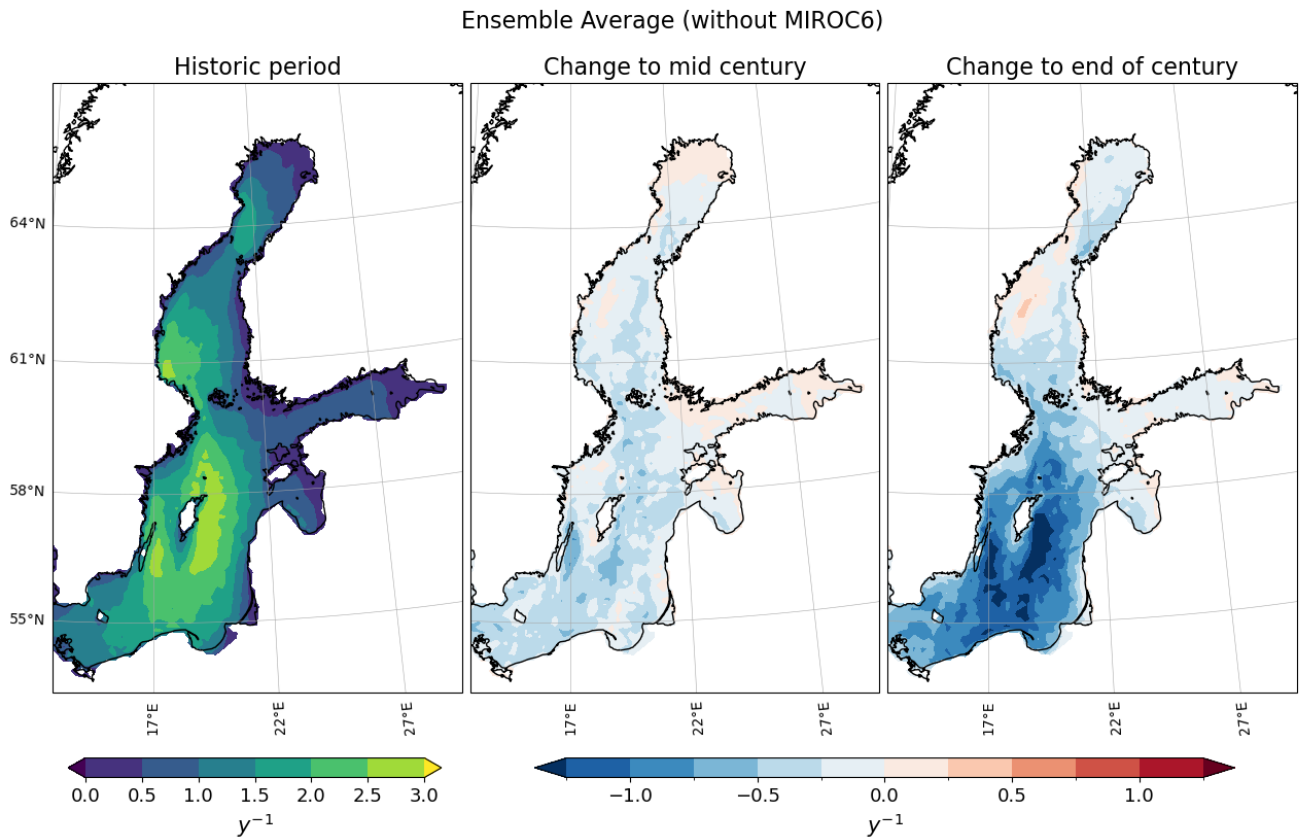


Figure B18: Number of snowband days per year and future change, ensemble average without the HCLIM12-MIROC6 simulation, here showing future - historic results.

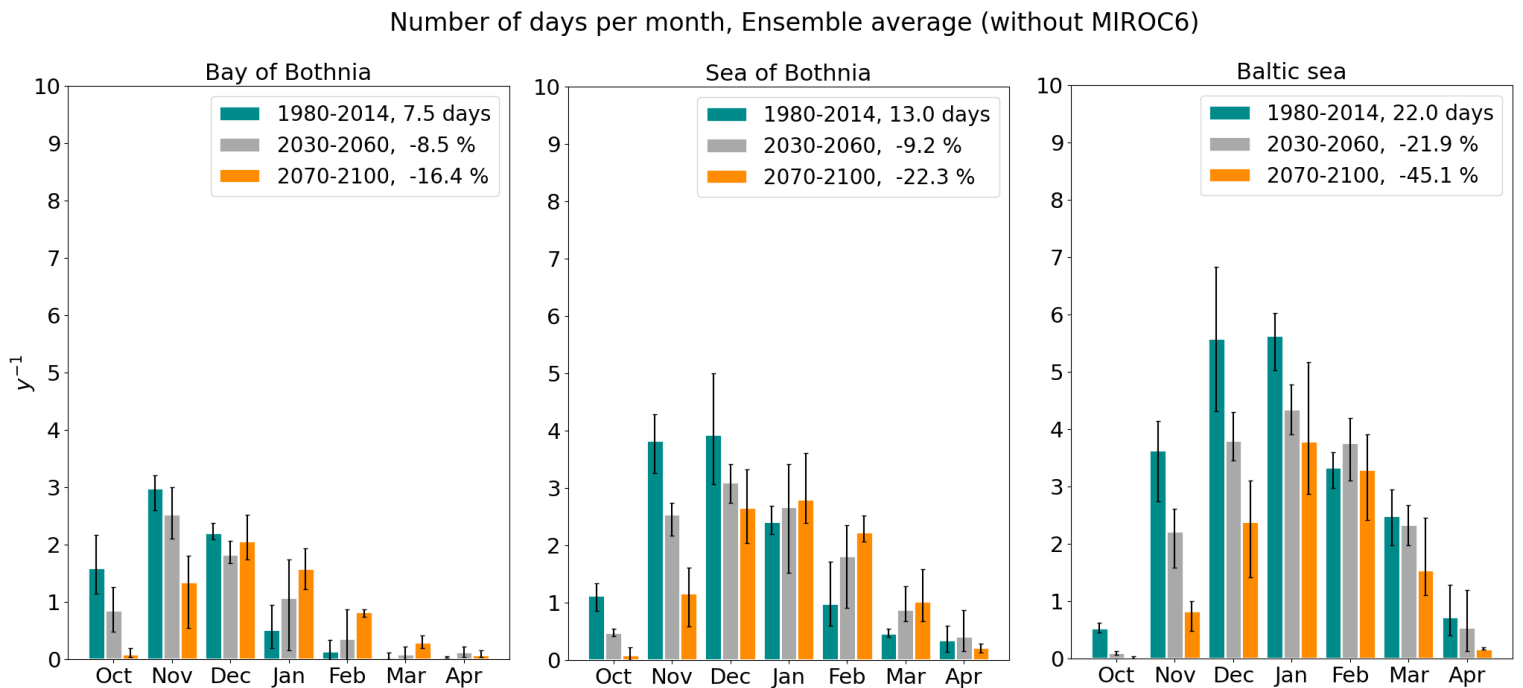


Figure B19: Number of snowband days per year and month, ensemble average without the HCLIM12-MIROC6 simulation. Errorbars showing the maximum and minimum value from the ensemble.

C Precipitation

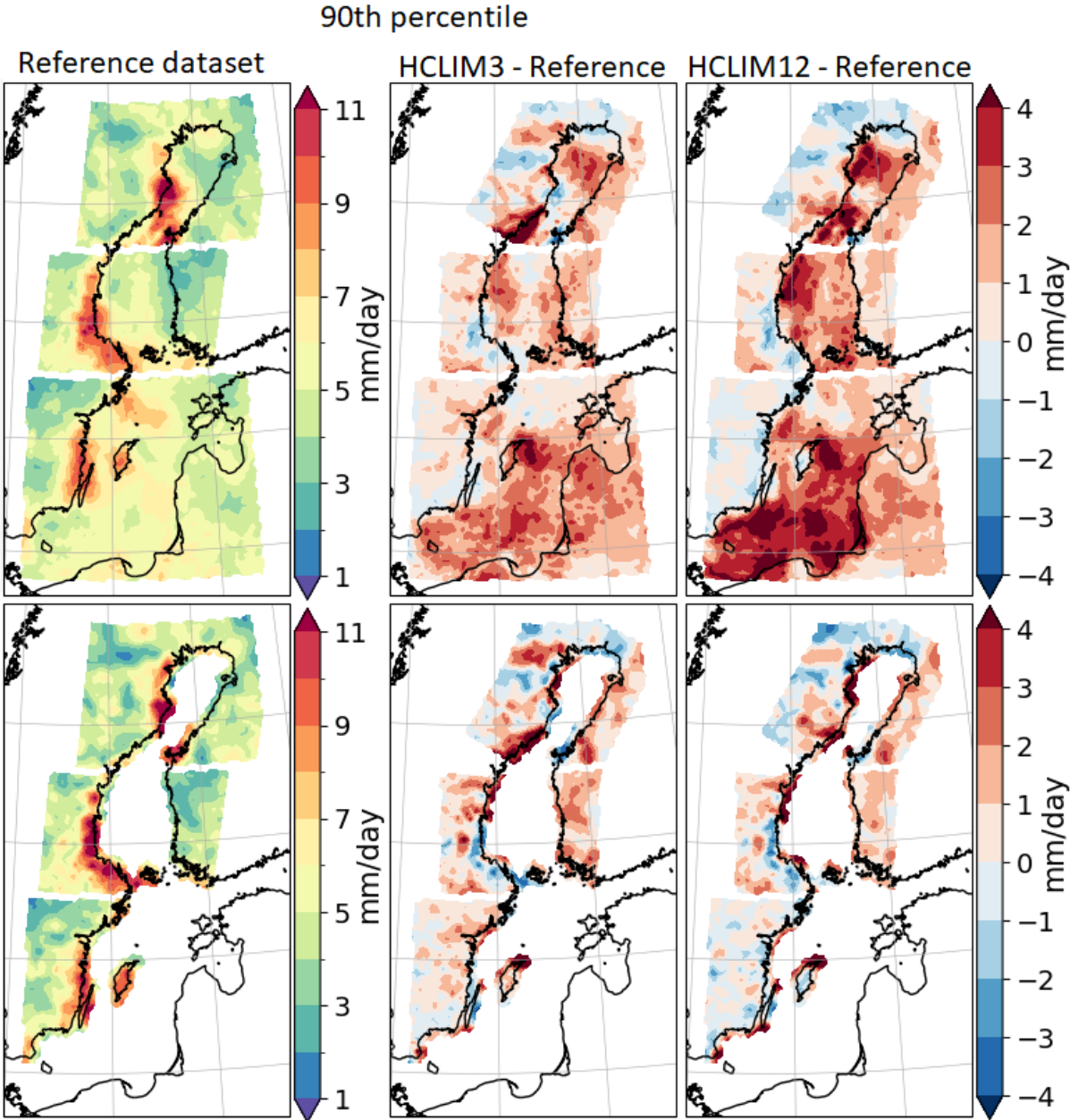


Figure C20: 90th percentile of total precipitation for all snowband days identified in both HCLIM3 and HCLIM12. Reference datasets; GridClim, top row, NGCD, bottom row, and the deviation in HCLIM3, HCLIM12 with respect to each reference. All precipitation datasets have been interpolated to the largest grid resolution.

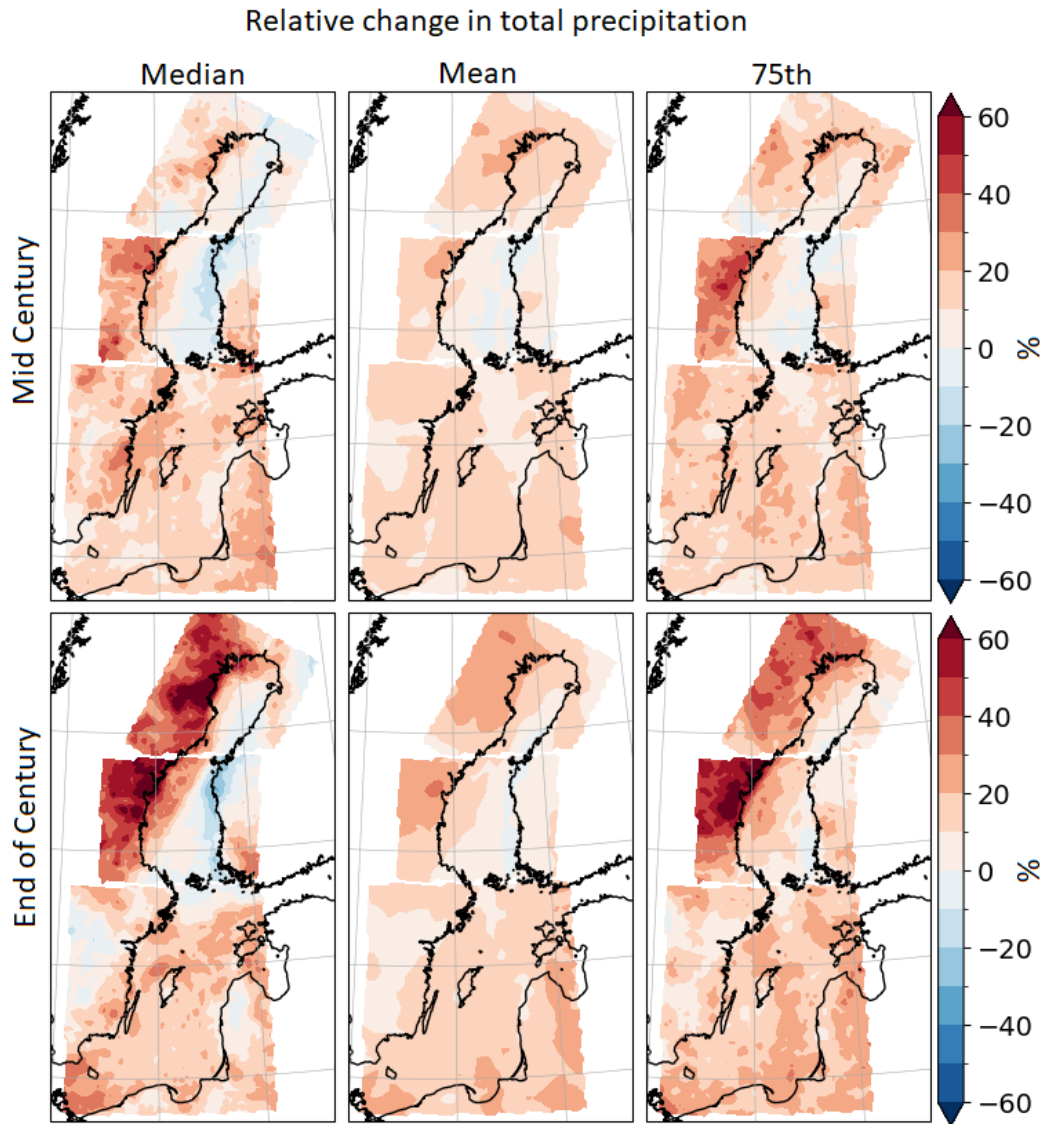


Figure C21: Relative change in the ensemble average of median, mean and 75th percentile of total precipitation for selected snowband days. Here towards mid century (2030-2060), top row, and the end of century (2070-2100), bottom row.

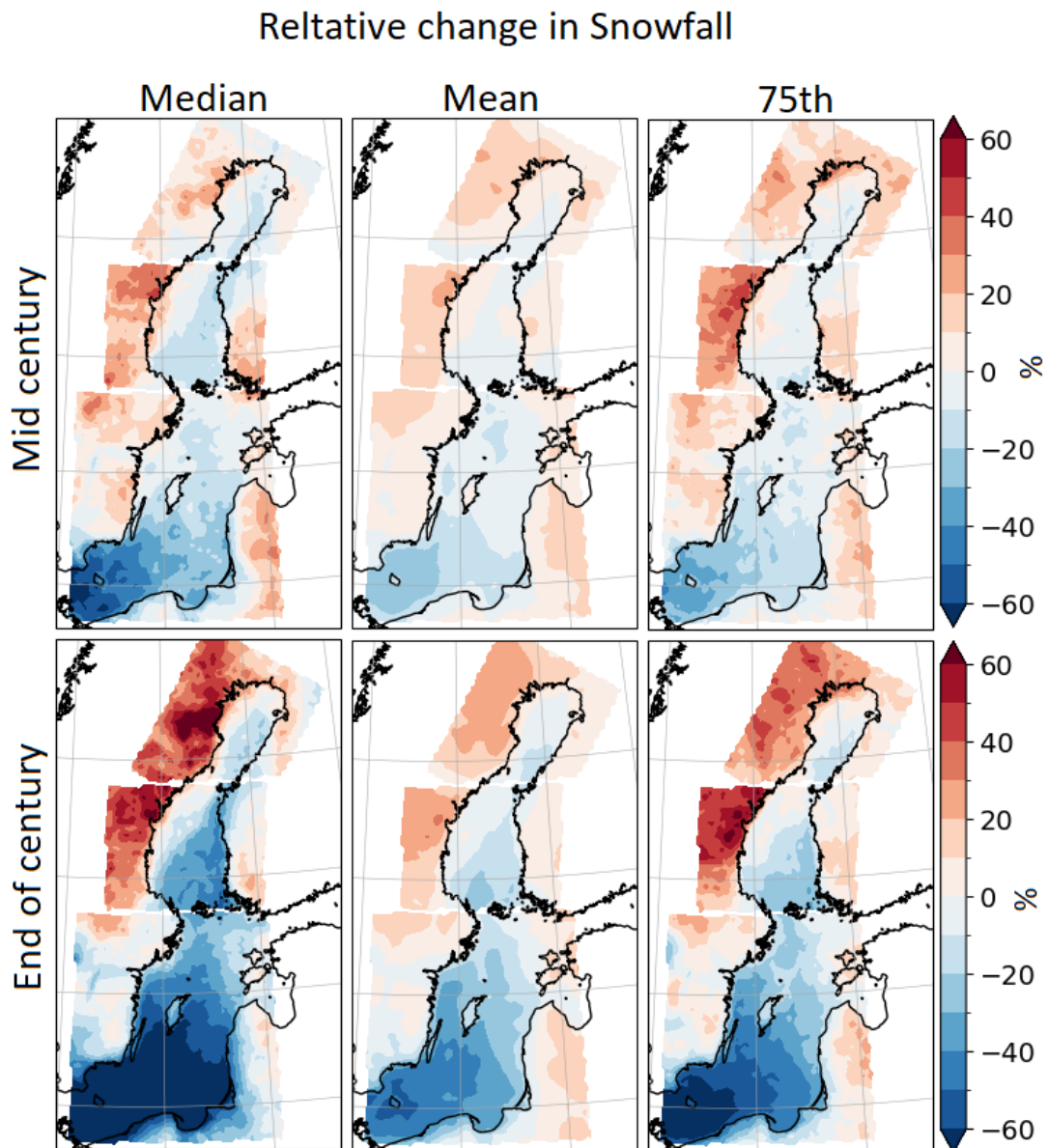


Figure C22: Relative change in the ensemble average of median, mean and 75th percentile of snowfall for selected snowband days. Here towards mid century (2030-2060), top row, and the end of century (2070-2100), bottom row.

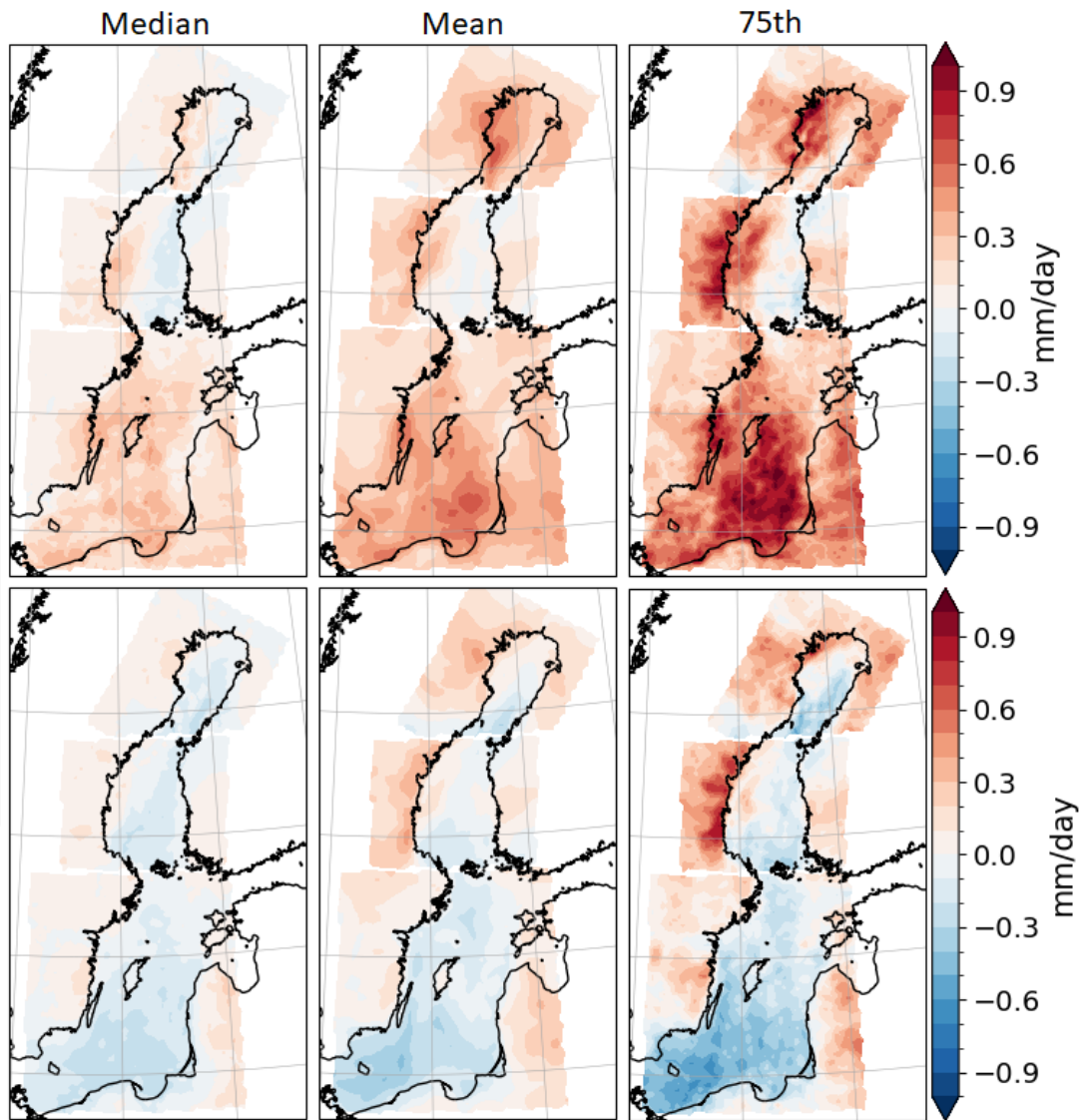


Figure C23: Change in the ensemble average of median, mean and 75th percentile of total precipitation, top row, and snowfall, bottom row, towards the mid century for selected snowband days. Here mid century (2030-2060) – historic (1990-2014).

D Meteorological Parameters

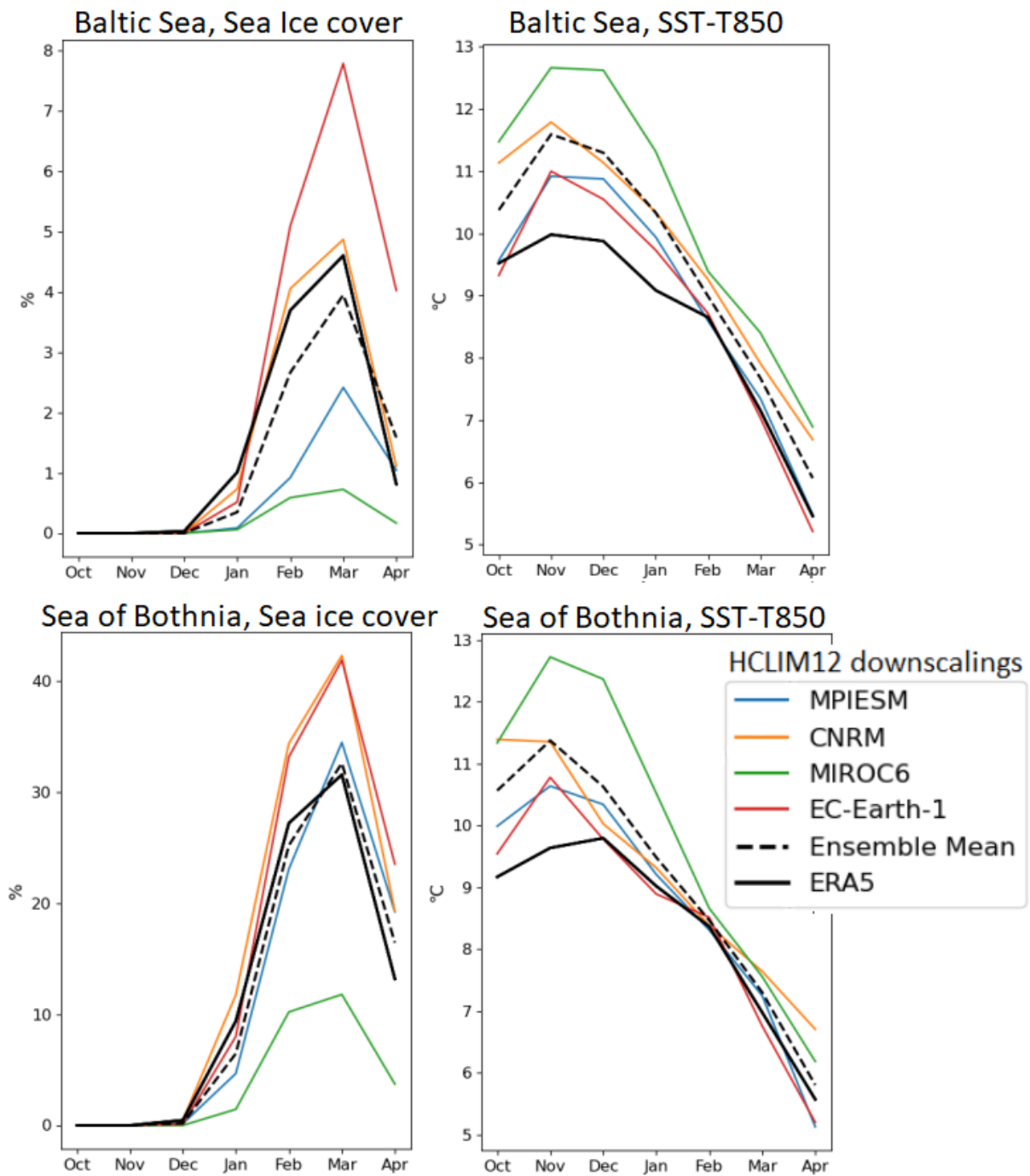


Figure D24: Monthly mean sea ice cover and temperature difference between the sea surface and air at the 850 hPa level for 1980-2014 in HCLIM12-GCM for the Baltic Sea and Sea of Bothnia.

Days exceeding threshold, HCLIM12 downscalings

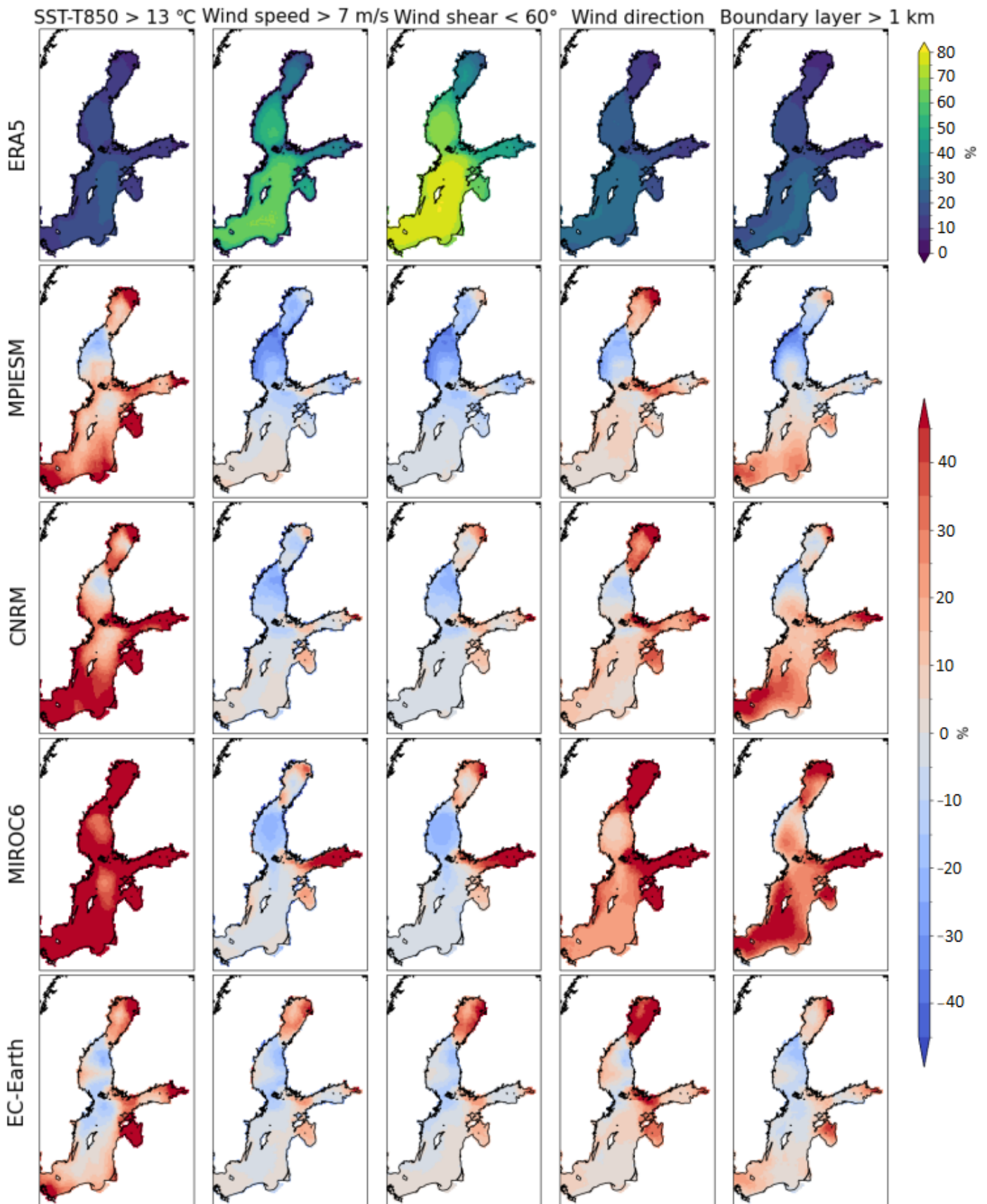


Figure D25: Top rows showing the percentage of days where parameter exceeds the snowband criteria for the HCLIM12-ERA5 simulation. Rows below showing the relative difference of that in the ensemble downscalings (HCLIM12-GCM).

Mean Sea Ice cover, HCLIM12-ERA5

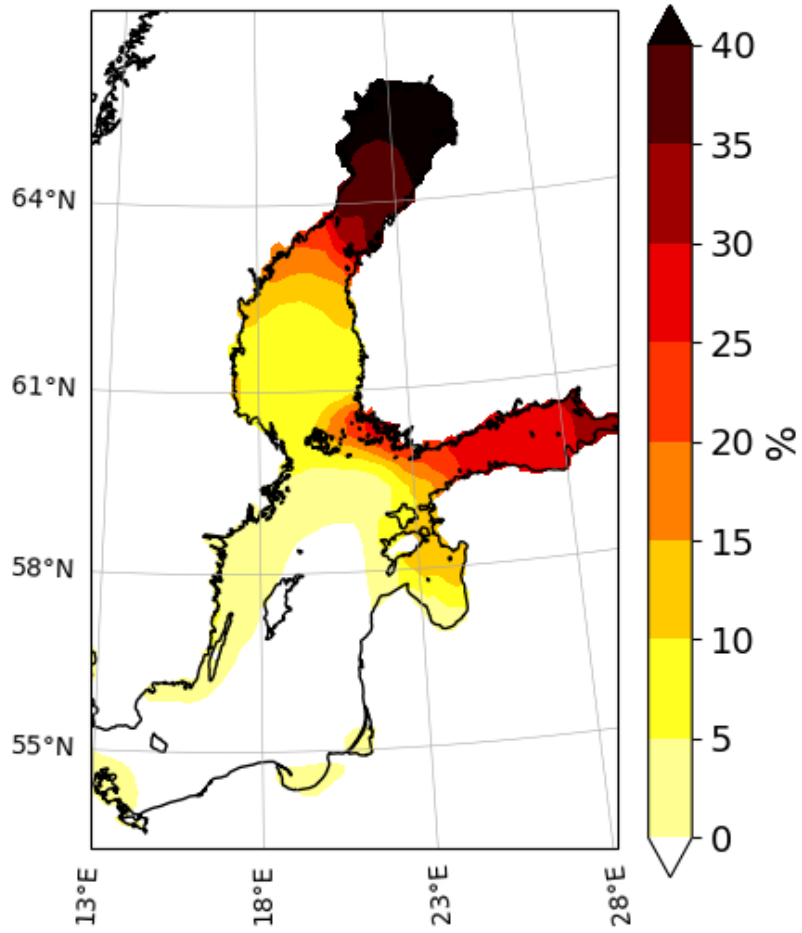


Figure D26: Mean sea ice cover for 1980-2014 in HCLIM12-ERA5.

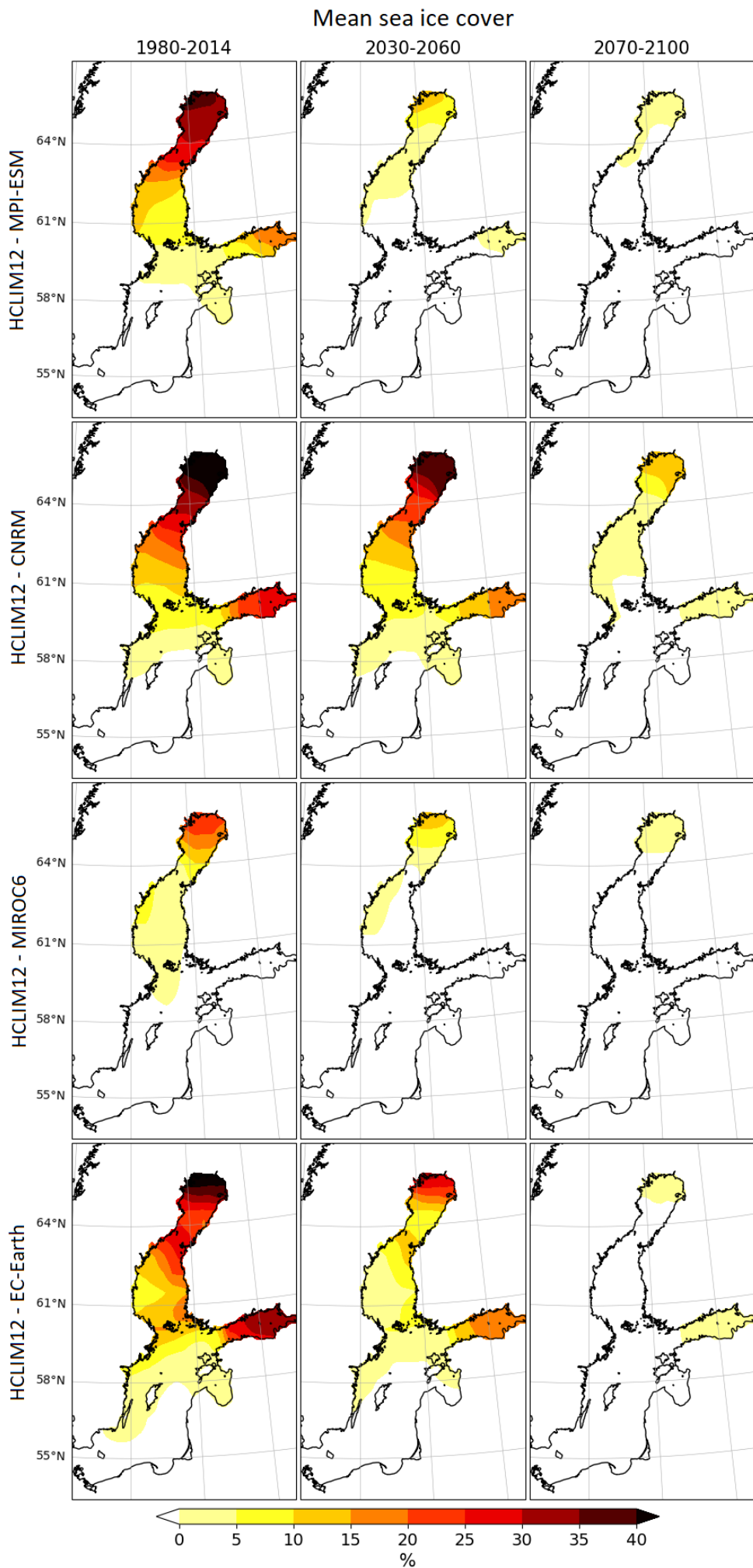


Figure D27: Mean sea ice cover for 1980-2014 and future projections in all HCLIM12-GCM.

Mean air temperature at 2 m

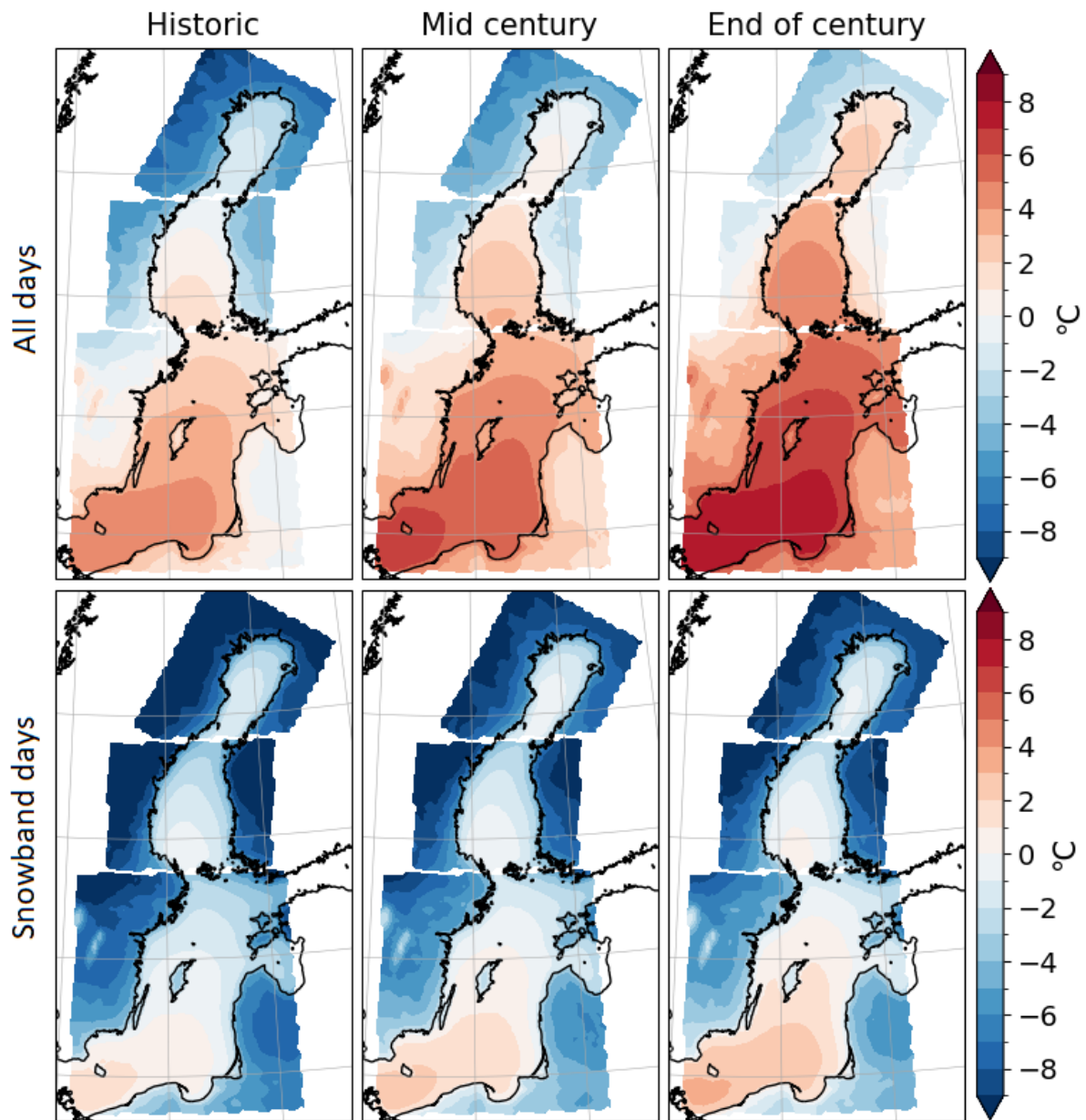


Figure D28: Average air temperature at 2 m height for all days, top, and identified snowbands days, bottom, for all simulated time periods; historic 1980-2014, mid century 2030-2060 and end of century 2070-2100. Results from HCLIM12-MPI-ESM and HCLIM12-CNRM.

Table D9: Ensemble average and standard deviation in parenthesis for gridpoints and 6h timesteps fulfilling all snowband criteria in the Baltic Sea area. Sign is shown when at least 75% of the ensemble demonstrate same sign in future change.

Baltic sea				
	1980-2014	2030-2060	2070-2100	Sign
ABL Height (m)	2196.6 (692.8)	2155.2 (689.5)	2111.3 (673.0)	-
SST (°C)	5.1 (2.3)	5.6 (2.1)	6.6 (1.8)	+
TempDiff (°C)	17.9 (2.6)	17.6 (2.4)	17.9 (2.4)	
Wind shear (°)	20.1 (15.1)	19.3 (14.7)	19.2 (14.6)	
Wind speed (m/s)	11.8 (2.8)	11.9 (2.9)	11.6 (2.6)	
Pr Sum (mm/6h)	2.6 (1.5)	2.8 (1.6)	2.9 (1.7)	+
Snowfall (mm/6h)	2.1 (1.3)	2.0 (1.3)	2.0 (1.3)	-

Table D10: Ensemble average and standard deviation in parenthesis for gridpoints and 6h timesteps fulfilling all snowband criteria in the Sea of Bothnia area. Sign is shown when at least 75% of the ensemble demonstrate same sign in future change.

Sea of Bothnia				
	1980-2014	2030-2060	2070-2100	Sign
ABL Height (m)	2069.2 (667.6)	2050.1 (651.7)	1937.3 (603.3)	
SST (°C)	4.5 (2.4)	4.6 (2.5)	5.1 (2.2)	
TempDiff (°C)	17.4 (2.3)	17.0 (2.2)	16.7 (2.2)	-
Wind shear (°)	21.1 (15.2)	21.0 (15.0)	20.8 (14.9)	-
Wind speed (m/s)	12.0 (2.9)	12.0 (3.0)	11.9 (2.8)	
Pr Sum (mm/6h)	2.9 (1.7)	3.0 (1.8)	3.1 (1.8)	+
Snowfall (mm/6h)	2.4 (1.5)	2.3 (1.5)	2.3 (1.5)	

Table D11: Ensemble average and standard deviation for gridpoints and 6h timesteps fulfilling all snowband criteria in the Bay of Bothnia area. Sign (+/-) is shown when at least 75% of the ensemble demonstrate same sign in future change.

Bay of Bothnia				
	1980-2014	2030-2060	2070-2100	Sign
ABL Height (m)	1881.1 (648.2)	1880 (625.0)	1751.1 (541.3)	
SST (°C)	4.6 (2.2)	5.0 (2.2)	5.2 (2.2)	
TempDiff (°C)	17.0 (2.4)	16.6 (2.1)	16.5 (2.2)	-
Wind shear (°)	24.2 (16.0)	24.3 (15.7)	22.3 (14.8)	
Wind speed (m/s)	11.9 (2.7)	12.1 (2.8)	11.6 (2.6)	
Pr Sum (mm/6h)	3.2 (1.7)	3.5 (2.0)	3.3 (1.8)	
Snowfall (mm/6h)	2.6 (1.5)	2.6 (1.7)	2.3 (1.4)	